Mechanistic modelling of Fatigue crack growth for metals

By:

TAWQEER ZADA
29-FET/MSME/S15

Supervised By:

DR. RAFIULLAH KHAN

DEPARTMENT OF MECHANICAL ENGINEERING, FACULTY OF ENGINEERING AND TECHNOLOGY INTERNATIONAL ISLAMIC UNIVERSITY, ISLAMABAD.

l

Thesis entitled

Mechanistic modelling of Fatigue crack growth for metals

Submitted to International Islamic University, Islamabad

in partial fulfillment of the requirements for

the award of degree of

MASTER OF SCIENCE IN

MECHANICAL ENGINEERING BY

TAWQEER ZADA

29-FET/MSME/S15

SESSION 2015-2018

DEPARTMENT OF MECHANICAL ENGINEERING

INTERNATIONAL ISLAMIC UNIVERSTY,

ISLAMABAD

DECLARATION

I, **Mr. Tawqeer Zada**, Reg. No. **29-FET/MSME/S15** student of MS mechanical engineering in Session 2015-2018, hereby declare that the matter printed in the thesis titled "**Mechanistic modelling of Fatigue crack growth for metals**" is my own work and has not been printed, published and submitted as research work, thesis or publication in any form in any University, Research Institution etc. in Pakistan or abroad.

Tawqeer zada:_____

Dated: 4/1/2018

Certificate of Approval

This is to certify that the work contained in this thesis entitled, **"Mechanistic modelling of Fatigue crack growth for metals"** was carried out by **Tawqeer Zada Registration# 29-FET/MSME/S15,** it is fully adequate in scope and quality for the degree of MS (Mechanical Engineering).
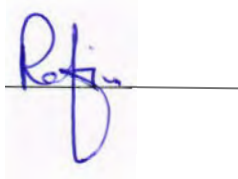
Viva Voice Committee

Supervisor

Dr. Rafiullah Khan

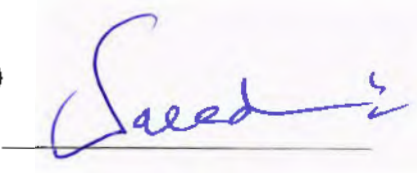Assistant Professor

DME, FET, IIU, Islamabad

Internal Examiner

Dr. Saeed Badshah

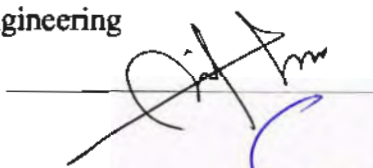Head of Department (HOD)

DME, FET, IIU, Islamabad

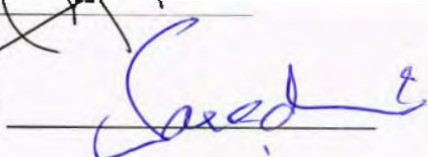**External Examiner**

Dr. Asif Israr

Head of Department (HOD)

Department of Mechanical Engineering
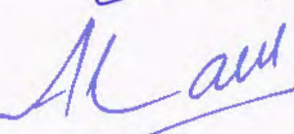
Institute of Space Technology

Chairman DME FET IIU, Islamabad

Dean FET, IIU Islamabad

Prof. Dr. Muhammad Amir

DEDICATION

I dedicate all my efforts to the **Holy Prophet Mohammad (S.A.W.),** who has been sent as a mercy to all mankind, my parents who have always supported me morally and financially, and have always prayed to Almighty ALLAH for my success, to my entire family members and to my respected teachers. I also dedicate it to my parents, brother and sister for their support and prayers.

ACKNOWLEDGEMENTS

ABSTRACT

Fatigue failure is the major causes of mechanical structural failure. The fatigue failure progress in three stages crack initiation, crack growth and final failure. The fatigue crack growth has been modelled by different approaches, however these approaches are generally empirical. In this research, a mechanistic fatigue crack growth model is proposed. The striation and its relation to the cyclic load is used for the model development. Scanning electronic microscope results are used to establish relation between striation and crack growth. The developed model is two-parameters. The model has been implemented and validated using experimental data from the literature. The model prediction is satisfactory in region II of the crack growth curve. However, in region I and region III the model deviates from experimental data. It is suggested to incorporate interaction of monotonic and cyclic loading in the mechanistic modelling for the fatigue growth.

Table of Contents

List of Figures

List of Tables

List of Abbreviations

LCF: Low cycle fatigue

HCF: High cycle fatigue

SIF: Stress intensity factor

SERR: Stress energy release rate

ASTM: American society of mechanical engineering

CTOD: Crack tip opening displacement

LEFM: Linear elastic fracture mechanics

SEM: Scanning electron microscope

FCG: Fatigue crack growth

MTS: Material testing machine

CT: Compact tension

Chapter 1

INTRODUCTION

1.1 Introduction

Fatigue failure occurs due cyclic loading. Fatigue failure is the major causes of mechanical structural failure [1]. The cost due to fatigue fracture in United State was investigated in 1978 was $119, which was 4% of total GDP. It gives importance to minimize this cost by using current and proper technology for designing of any mechanical structure[2]. Few examples of different mechanical structures failure due to fatigue are shown in figures 1.1 and 1.2 respectively.
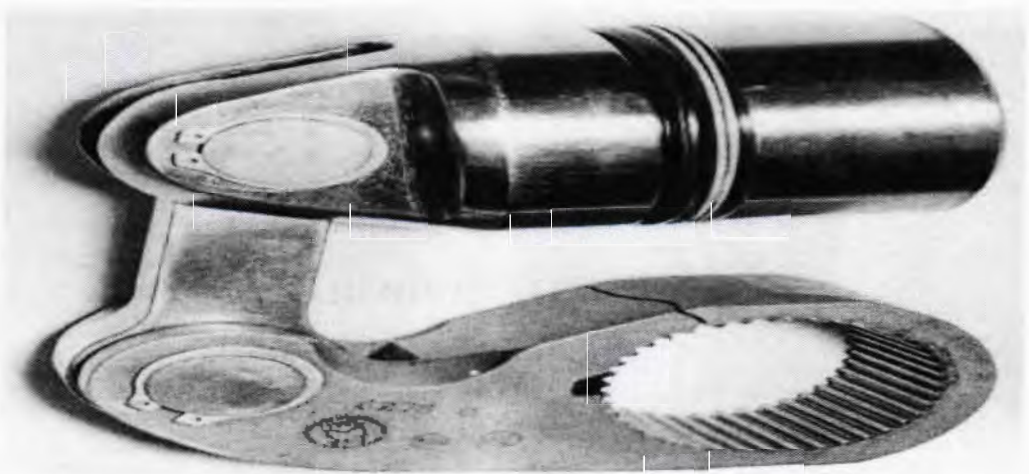
Figure 1.1: Fatigue crack originating at spline [3]
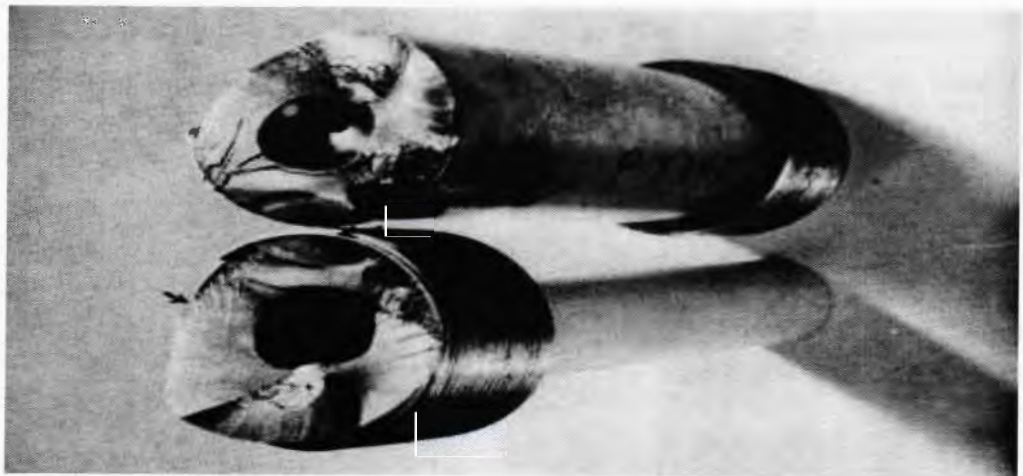
Figure 1.2: Fatigue in landing gear bolt [3]

Fatigue failure occurs in a mechanical structure in three phases crack initiation, crack growth and finally rapid fracture [4] as shown in figure 1.3.
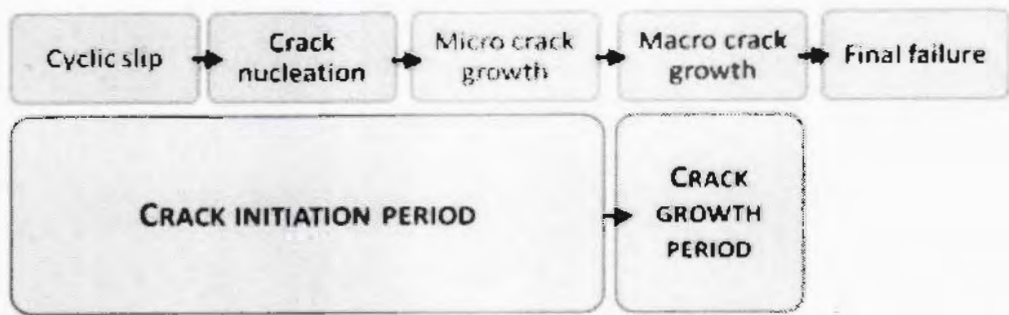
Fig 1.3: Various stages of FCG [5]

Crack initiation is the early fatigue damage occurs at the point of maximum stress concentration factor. This phase is controlled by stress concentration factor [6]. Then crack initiation is followed by crack growth. Crack growth is the macroscopic phase of fatigue life reported by various researchers [7, 8].

The analysis of crack growth has been done by using fracture mechanics parameters such as J-integral, energy release rate and stress intensity factor. Different crack growth models have been developed for the prediction of this regions. For example, Paris [9] correlate SIF with crack growth in his model. Empirical as well as an analytical modelling has been developed by various researchers.

1.2 Problem Statement

The existing approaches are generally developed empirically. The physical mechanism of the crack growth has not been well defined and incorporated into the crack growth models. In essence, the crack growth takes place due to plastic flow of the material promoting crack closure. The crack growth behavior can be explained by the plastic deformation and disbanding at the crack tip. The present knowledge of the fracture surface under fatigue and huge experimental data can be used for the development of a mechanistic fatigue growth model. The mechanistic model will end the hurdles of the stress ratio effect and variable amplitude effects on the crack growth.

1.3 Research Objective

The objective of this thesis is to develop a mechanistic crack growth model for metals and its implementation and validation by using fracture mechanics approach.

1.4 Research Methodology

The mechanistic model for the FCG in metals has been developed using analytical approach. The existing empirical, semi empirical and mechanistic models have been critically analyzed in the first part of research. The fractographic observation of the FCG in the existing literature has been used to depict realistic pictures of fatigue crack growth phenomenon. The

2

observation has been used to establish relationship between dependent and independent variables of the FCG phenomenon. A mechanistic model has been proposed accordance to the observed FCG phenomenon. The model has been implemented using experimental data of fatigue growth rate obtained from authentic literature resources. MATLAB software has been used for the determination of the model parameters using its surface and curve fitting tool boxes. The model has been validated using experimental data from other literature resources.

1.5 Thesis scope and organization

In this research work, a mechanism based model has been developed using fractographic observation. Striation marks relation has been used to establish relation between crack growth and loading. A two-parameters model is proposed for the FCG. The model has been implemented and validated using experimental data from literature. The next chapter is the literature review about the existing mechanistic models for the fatigue crack growth. Chapter 3 described the mechanism for the development of the proposed model. Chapter 4 described implementation and validation of proposed model. Chapter 5 described discussion. Chapter 6 is about this dissertation the conclusion and the future recommendations.

CHAPTER 2

LITERATURE REVIEW

This chapter covers the literature review of the different Fatigue Crack Growth Models developed analytically by the various researcher for metals. Every Model have their own consequences about the mechanism of Fatigue Crack Growth. Here we briefly discuss multiple Models to know about the existing analytical approaches to understand better about the FCG mechanisms.

<u>Overview of literature on mechanistic modelling of FCG in the following table 2.1:</u>

Authors	Fatigue crack growth model	References
Tomkins, B.	$\frac{da}{dN} = f(\Delta K, \Delta\varepsilon_{plastic} \cdot r_{plastic}^{cyclic})$	[10]
Lal, D. N. et. al	$\frac{da}{dN} = a(\frac{\sigma N}{\sigma FF})^{\frac{nF+1}{nF}} \cdot f(a/w) - \frac{\rho^* F}{2}$	[11]
Chan, K. S. et. al	$\frac{da}{dN} = C_1 \Delta K^n [1 - (1 - \frac{\tau_B}{\tau_A})(\frac{D-2X}{D})^m]$	[12]
Suresh, S.	$\frac{da}{dN} = f(\Delta K, \theta_{deflect}, L_{deflect})$	[13]
McEvily, A. J. et. al	$\frac{da}{dN} = A(\{\sqrt{\frac{\pi\rho_e}{4}} + Y \sqrt{[\frac{\pi}{2} a (\sec\frac{\pi\sigma}{2\sigma_y} + 1)]}\}\Delta\sigma - (1 - e^{-kl})K_{opmax} - \Delta K_{effth})^2$	[14]
Krausz, A. S. et. al	$\frac{da}{dN} = f(T, U_{reverse}, U_{forward}, \Delta K, V^*)$	[15]
Lichun Bian et. al	$\frac{db}{dN} = \frac{G_{cr}f \cdot (\Delta K_1, \Delta K_2, \theta_0)}{(G_{cr} - \Delta G_{max})\partial_{yld}^2}$	[16]
Schweizer, C. et. al	$\frac{da}{dN}\big|_{block} = \frac{da}{dN}\big|_{total} + \sum_{blocl}\frac{da}{dN}\big|_{HCF}$	[17]
Maierhofer, J. et. al	$\frac{da}{dN} = C.F \frac{(\Delta K - \Delta K_{th})^m}{1 - \frac{1}{1-R}\frac{\Delta K}{K_C}}$	[18]
Shan Jiang et.al	$\frac{da}{dN} = C(\Delta K_{eff})^m$	[19]

2.1 Tomkins Model

Tomkins[10] proposed this model to predict the fatigue crack propagation due to de-cohesion of material near crack-Tip. The stage II propagation process of crack in ductile material under tension-compression loading as derived by Tomkins. The theory was purely based on slip based de-cohesion. This approach was used for the various fatigue problems. Tomkins found that FCG rates depend on materials stress-strain behavior of their control size and its deformation zone at the Tip of crack. By increasing the limit of strain to the limit of tensile strain, so new surface of crack is formed due to de-cohesion of shear toward inner edge of flow band where the gradient of shear is more. During unloading the tensile and loading into compression thus shear flow become reversed and the crack close without any re-cohesion and the shear stress distribution at the crack-Tip is at ±45 as shown in fig 2.1.
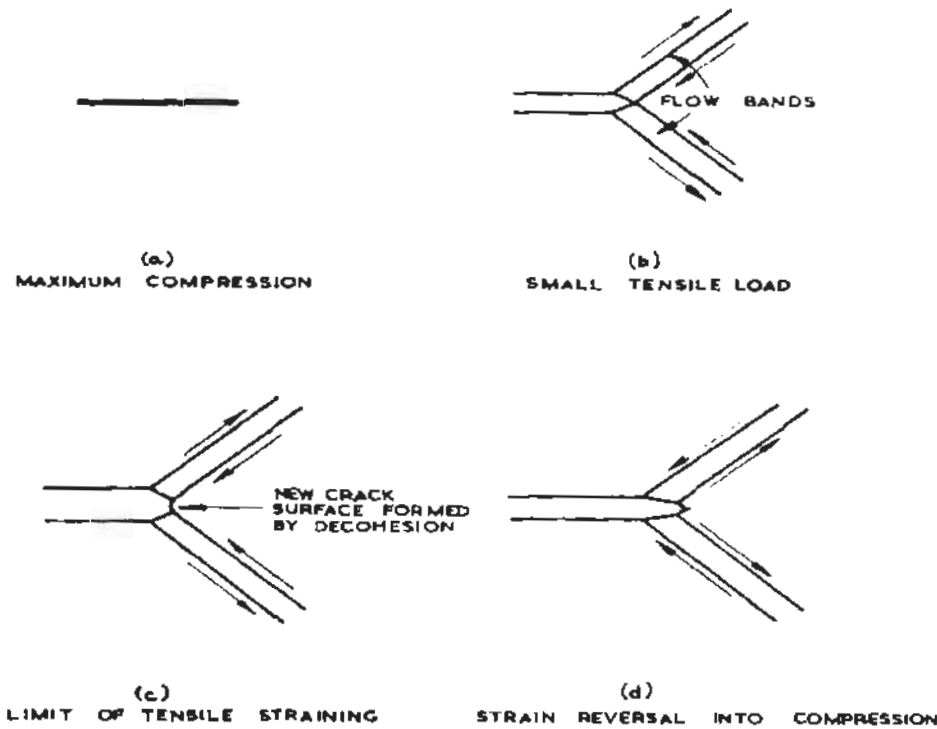
Figure 2.1: Stage II FCG mechanism in a metal [10].

The primary input of this Model was size of cyclic plastic zone , $r_{plastic}^{cyclic}$ and plastic strain range, $\Delta\varepsilon_{plastic}$.

$$\frac{da}{dN} = f(\Delta K, \Delta\varepsilon_{plastic}, r_{plastic}^{cyclic}) \tag{2.1}$$

ΔK range of stress intensity factor, $\Delta\varepsilon_{plastic}$ range of plastic strain and $r_{plastic}^{cyclic}$ represent plastic zone size.

The above mechanism gives the picture about fatigue crack growth that by applying tensile load to the pre-crack material thus plastic zone create at the crack-Tip. And then crack begin to propagate toward de-cohesion plane and at any instant of crack propagation a new surface is formed at the crack-Tip. In short, Tomkins considered the period II process of FCG in more detail and concluded that at maximum shear plan de-cohesion result a new surface is formed. Through the above model fatigue crack growth failure was derived theoretically for both low stress region and high stress region, also determined the material parameter controlling crack propagation. The above model confirms the universality of Coffin Manson law for the fatigue criteria above endurance limits.

The above model was derived for the stage II FCG with mode I but not considering the stage I crack growth with mode II, similarly his focus was on the uniaxial fatigue crack growth data and doesn't incorporate multiaxial fatigue crack data [20] . This approach lacking stage I FCG, not succeed to develop such an analytical based model apart from fracture mechanism of stage II [21]. The above model just incorporated characteristic of stress-strain but not succeed due to considering structural parameter because the model was based on slip plane based de-cohesion [11]. The above model was developed only for ductile material but not exceeded for the FCG of brittle materials[10].

2.2 Lal and Weiss Model

Lal and Weiss [11] proposed Fatigue Crack Growth Model which utilizes the recent progress in the notch analysis due to fracture and also utilizes the size effect concept which result from the variation in the stress volume of the Crack-Tip. Accordingly, mechanism of Fatigue Crack Growth involves local stresses which is reaching to the theoretical cohesive strength that causes fracture of atomic bond near threshold at the relevant nominal stresses. Whereas plastic blunting, slip plane de-cohesion and Crack-Tip re-sharpening may occur when the stress range is above threshold range as shown in fig 2.2.
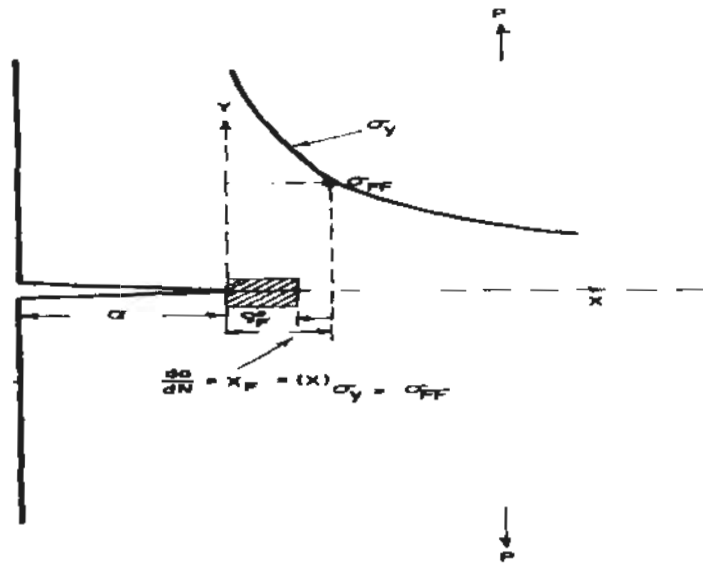
Figure 2.2: Schematic diagram of FCG mechanism [11].

The following equation was proposed:

$$\frac{da}{dN} = a\left(\frac{\sigma N}{\sigma FF}\right)^{\frac{nF+1}{nF}} . f(a/w) - \frac{\rho^* F}{2} \qquad (2.2)$$

$\frac{da}{dN}$ is the crack growth, a is the crack size, σFF *and* σN are the local fracture stress, nF represent local strain of hardening exponent, $\rho^* F$ Neuber structural constant, $f(a/w)$ is the dimensionless correction factor. The Model composed of three important parameters like σFF, nF and $\rho^* F$. All these three parameters have physical importance and an accommodate conventionally material strength effects, structural inhomogencity and stress-strain behavior. Thus, from the above approach we get better understanding of the whole crack growth curve. As the approach was based on notch analysis, the condition of crack initiation, crack propagation also analyses the non-propagation of cracks from machine notches.

The above model shows a linear relationship between crack growth rate and crack size and also the model gives accurate data trend in the whole crack growth curve. Fatigue fracture surfaces show us that the changes occur in the micro-mechanism is due to striation mode.

The above model has been developed to investigate the notch analysis during fatigue crack growth by using fracture approach. In their investigation, it was found that every element experience cyclic stress and strain of size ρ^* ahead the crack-tip are determined with the help of elastic-plastic approach. It was found in his model that ρ^* parameter (Neuber structural constant) have been used but has no direct physical assessment method have not been developed for this parameter. Also, it was not clear that is it possible to simulate fracture

7

mechanism near crack-tip due to cyclic deformation of smooth specimen [22]. The process of fatigue growth of macrocrack is due to the repeated act of fracture certain elementary volume ahead the crack-tip of size ρ^*. This process is simulated by fracture having smooth specimen of the relevant material. But the duration of this mechanism is determined by using the relevant low cycle fatigue diagram. By using this criterion, it is suitable to analyses the similarities in the fracture and deformation process ahead the crack-tip running with the same process of smooth specimen. However, the physical meaning of this parameter ρ^* is not clear and are not method for direct evaluation[23]. The above model show good response in-case of uniaxial loading characteristics but was not extended for mixed mode cracks characteristics and also incorporated the effect of surface frictional [24]. The above approach was developed for stage II and model limit was up-to m=2 also not include stage III and lacking physical insight with crack growth process[25].

2.3 Chan and Lankford Model

Chan and Lankford [12] modified the linear elastic fracture mechanic approach to consider the grain boundaries effect and the variation due to grain orientation effects. This analytical model was proposed basically on the deduction that for long crack near threshold the stress intensity factor, the CTOD is greater for small crack with respect to the equivalent long crack. Plastically the strain range for long crack is smaller with respect to the small crack. Assuming the effects of different parameters like neighboring grain orientation as well crack-tip distance from nearest grain boundaries are describing by the following equation:

$$\frac{da}{dN} = C_1 \Delta K^n [1 - (1 - \frac{\tau_B}{\tau_A})(\frac{D-2X}{D})^m] \qquad (2.3)$$

C_1, n, m are constants estimated experimentally, $\frac{da}{dN}$ represent rate of crack growth, ΔK represent range of stress intensity factor, τ_A and τ_B are the resolved shear stresses of grain A and grain B, D is the diameter of grain and X show the distance from grain boundary to crack-Tip.

In the above model, it was seeming that the fatigue behavior of long crack is different from short crack in engineering alloys. It was also observed that physically small crack is in the order of micrometer in size which is nucleated at the inclusion of grain. For the short crack-Tip the plastic deformation is manifested by localized slip band inclined to the stress axis which are restricted to the region where the stress intensity dominates at the Crack-Tip. From this approach, we get that the local plasticity at the tip of crack is basically used for the measure of

fatigue damage. This approach was based on concept, if greater the plasticity at the tip of small crack, thus crack-tip opening displacement occurs at the tip of small crack compatible to the relevant rapid growth of equivalent long crack. The deduction of strain range of crack tip at the grain boundary show deacceleration in the growth rates of microcrack. But if there are similarities in crystallites of both small and long crack-tip strain range, the model predicts no deacceleration.

The above model was based on the criteria that the short crack growth rate is maximum than the growth rate predicted by the linear elastic fracture mechanics approach in the early stages and finally slow down the growth rate compare to the growth rate of long crack. But the proposed model was not experimentally verifying to determine the plastic range at the crack-tip of large crack and small crack. The proposed model also not explain the transition from short crack to long crack, because for the transition two parameters are required in the form of work hardening and grain boundary effects. But the present model does not consider the effect of work hardening [26]. The above model considering the LEFM approach for the analysis of short crack. Since LEFM approach is not suitable in case of short crack application, the ΔK criteria become questionable in the short crack analysis [27]. In this model, the influence of microstructure on short crack was describe and other parameters were also described like the diameter of grain as well as the accurate position of crack-tip near to boundary of grain. But the model was fail due to not incorporated the application of crystal plasticity theory [28]. The model doesn't describe the FCG of small crack satisfactorily, because of observing mark scattering during crack growth. It calculates low deceleration or no deceleration during FCG rates in the cases of two homogenous grains when a crack grow through the boundary of theses grains [29].

2.4 Suresh Model

Analytically, many researchers trying to predict crack growth of materials with respect to the crack path of its geometry. Suresh [13] equation explain the reduction of fatigue crack growth rate was because of periodic deviation from their straight path and due to the associated attachment of flanks. This deflection in the crack path is due to stress state, microstructure discontinuities, environment, grain boundaries and variation in loads. The basic assumption was that the crack requires maximum load in the form of driving force, like ΔK which propagate the crack of same length. He shows that the crack growth rate for such crack path depends on ΔK, $\theta_{deflect}$, $L_{deflect}$.

$$\frac{da}{dN} = f(\Delta K, \theta_{deflect}, L_{deflect})$$ (2.4)

ΔK is the range of stress intensity, $\theta_{deflect}$ angle of crack deflection and $L_{deflect}$ represent the length deflected from actual path.

It was found that if crack show deviation from their actual path, so it means at the crack-Tip both sliding displacement and tensile opening occurs even the load we have purely tensile. It was found if crack is subjected to both shear load and tensile load at the crack-Tip we have Mode I and Mode II and its corresponding value of K_I and K_{II} at the Tip of crack which is deflected will be the function of the relevant stress intensity factor for the same length of linear crack as show in fig 2.3.

Figure 2.3: Crack deflection mechanism for linear crack [13].

But deflection due to mixed mode cyclic loading is very severe. Experimentation show us that due to mixed mode stresses superimposing externally decreases, increases or remain unchanged the rate of propagation with Mode I FCG.

Suresh analyses in his model that how crack deflection influences the growth of short and long fatigue cracks during tensile loading. His focus was on the deflection in crack path due to Mode I cyclic loading in his approach.

In the above model, the effects of crack deflection on fatigue crack growth of mode I was examined. The theoretical understanding of crack deflection mechanism is a very complex problem. To-date not such a model has been developed to justify the crack growth behavior whose based was on the interaction of deformation process and crack deflection. This approach also not analyses the crack growth behavior because it's based was only on mode I [30]. Suresh show that for a small crack there is a little deflection, thus the value of K is varied crack to crack, but in-case of long crack the variation in the value of K is consistent. The model was unable to describe FCG rates of small crack by using the argument of deflection. Also, it is not possible to seem without one postulate dependent highly on the value of K_{II} [31]. He doesn't

incorporate some important factors like secondary crack and crack-tip branching in his model [32].

2.5 McEvily et al Model

McEvily et al [14] developed model for the analysis of short cracks incorporating plasticity effect, FCG threshold and crack closure. The behavior of small crack fatigue doesn't analyzed by linear elastic fracture method due to large size plasticity effects and disintegration occurs for both the correlated stress intensity factor and FCG rates of crack length having less than in size a millimeter. So, in the present approach some of the modification are carried into the linear elastic fracture criteria to introduce such parameter, that correlating both short and long FCG rates data. The new parameters in the present model used only for the behavior of short FCG rates comparing with empirical data.

Following equation was proposed:

$$\frac{da}{dN} = A(\{\sqrt{\frac{\pi \rho_e}{4}}) + Y \sqrt{[\frac{\pi}{2}a\left(\sec\frac{\pi\sigma}{2\sigma_y} + 1\right)]}\}\Delta\sigma - (1 - e^{-kl})K_{opmax} - \Delta K_{effth})^2 \qquad (2.5)$$

$\frac{da}{dN}$ represent crack growth rate, A show the empirical constant, l represents short crack length, K_{opmax} represent long crack opening, K represent the parameter in mm^{-1}, ΔK_{effth} represent effective stress intensity factor range, a show crack size, σ_y represent yield strength, σ represent applied stress, Y represent geometry factor and ρ_e represent the empirical parameter determine experimentally.

It was found by this approach that there are some characteristics which differentiate long crack behavior from short crack behavior. First one is the size of plastic zone at the tip of short crack is large comparatively to crack length, which is violation in term of LEFM approach. Second characteristics is the level of applied stress range may be maximum relative to material yield strength which show again violation according to LEFM approach at small scale yielding. Third one is crack closure range during transition period when small crack transformed to long crack. Crack closure decrease range of effective stress intensity factor, so therefore maximum driving force is needed for the FCG rate of small crack with respect to long crack for the same stress level. As the FCG rate of small crack is maximum than long crack. Finally, it is found that FCG behaviors of short crack will be calculated with help of LEFM expression in term of stress intensity factor. The procedure of analysis developed is capable for FCG of both short crack and long crack.

The above model proposed for the analysis of short cracks incorporating plasticity effects, crack closure and the crack growth threshold. The above model estimate the crack growth behavior but doesn't deal the usual deacceleration and accelcration behavior of short surface fatigue cracks, because the LEFM approach is un suitable for the application of short cracks [27]. In the above approach, the endurance limit was not considered rather than crack growth threshold level for the controlling of crack growth in the very short crack growth range [33]. The model was succeeded in-case of uniaxial loading but not showing good response during multi-axial loading of fatigue problems [34]. As we know that the above model was proposed based on crack closure but there was a very little number of empirical data which verified the present model [35].

2.6 Krausz Model

Krausz [15] proposed the idea of trans-granular FCG approach was based on slip reversal where the crack growth rate of trans-granular is comparable to the range of plastic strain at the Tip of crack. The role of slip system due to which fatigue damage occur has been recognised. Fatigue damage both initiation and propagation is due to the slip dislocation. The slip reversal is responsible for the crack vertex sharpening. The alternating slip reversal process and the forward slip process also carry the formation of striation during crack propagation. The model for the trans-granular crack growth rate is explain as follow:

(1) By applying load, the slip system activated in two orientations along the slip plane S1 as well slip plane S2.

(2) During S1 loading cycle purely forward slip occur, which develop a slip step whose length is l_f.

(3) During unloading a slip reversal occur of length l_r on S1.

(4) Finally, a slip reversal occurs on S2 which producing the crack tip sharp. The process is repeated until several loaded cycles by producing the final crack size (a). Similar process is repeated for another slip system having pair of parallel slip panes (S3 and S4) as shown in fig 2.4.
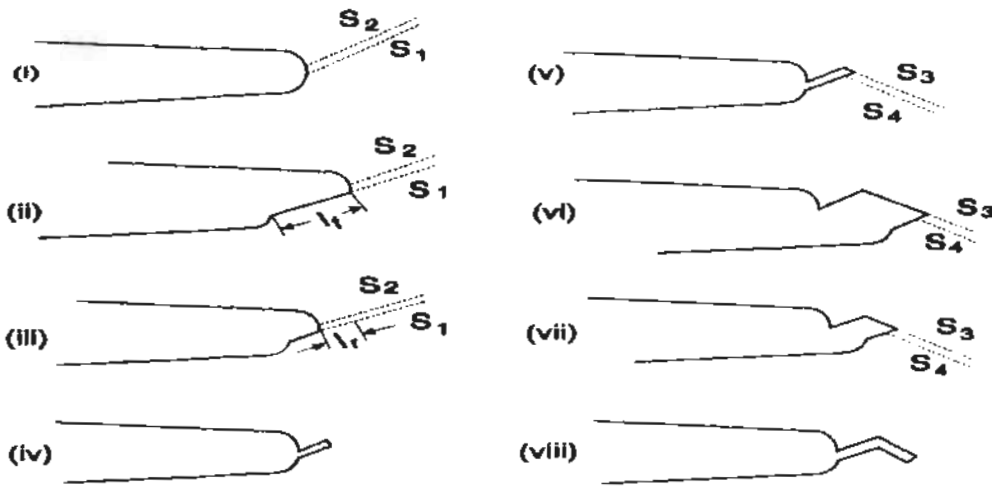
Figure 2.4: Schematic diagram of FCG by restricted slip reversibility [15].

This mechanism is repeated for every cycle. The following model was proposed:

$$\frac{da}{dN} = f(T, U_{reverse}, U_{forward}, \Delta K, V^*) \tag{2.6}$$

$\frac{da}{dN}$ represent the crack growth Rate, T represent absolute temperature, $U_{reverse}$ as well $U_{forward}$ represent reverse and forward displacement, ΔK represent stress intensity factor range and V^* represent activation volume.

The above model shows explicitly of FCG rates in the form of different material properties like work hardening coefficient, yield strength, microstructure quantities like activation energy, activation volume, as well as R and ΔK.This Model gives a physical mechanism for both crack initiation and crack growth processes and provides a physical description about striation formation during FCG results in trans-granular fracture. The Model proposed to correlate trans-granular FCG with plastic deformation which accommodate at the crack-Tip.

The above model was developed by combining the RSR with linear elastic fracture mechanics to developed FCG model of trans-granular type only for polycrystalline isotropic materials, but was not successful for the texture materials of different alloys [36]. His model was not able to estimate both the threshold regime and Paris regime [37]. The model doesn't consider material texture effect on FCG rates [38].

2.7 Lichun Bian and Farid Taheri Model

Farid Taheri et al [16] proposed this model to investigate the G_{max} approach based on the principle of elastic strain energy and extended to study the FCG mechanisms of mixed mode cracks. Some modification has been account to this approach to implement the plastic stain energy thus a new elastic-plastic model is presented based on energy. The proposed model incorporates the plastic zone at the tip of crack whether yielding take place. Because plastic zone is the parameter to control the crack extension in the elastic-plastic solid. The following model was proposed:

$$\frac{db}{dN} = \frac{G_{cr} f'(\Delta K_1, \Delta K_2, \theta_\circ)}{(G_{cr} - \Delta G_{max}) \partial_{yld}^2} \tag{2.7}$$

$\frac{db}{dN}$ represent crack growth size, ΔG_{max} represent release rate of strain energy, ΔK_1 *as well* ΔK_2 represent corresponding stress intensity factors range, G_{cr} represent critical value of strain energy rates, ∂_{yld}^2 is the material yield strength, $\theta_\circ$ represent radius of plastic zone at tip of crack and f' represent function of angle.

Advantage of the above model was comparative to another model doesn't required to determine C and m experimentally. That's why it enables to predict fatigue life without first finding the experimental constants. The above model show improvement with respect to other existing models because its predict fatigue life with mixed mode also.

The above model doesn't consider interaction of fractional surface during FCG so as a result the proposed model show doesn't a good agreement with the experimental data, therefore the model is not much effective for the estimation of fatigue life [39].

2.8 C. Schweizer Model

C. Schweizer et al [17] proposed mechanistic model based on the evolution of microcrack under lower cycle Fatigue and combine lower and high cycle Fatigue loading condition. Because we know various engineering structures are under the combine effects of LCF/HCF loadings. During lower cycle fatigue loading larger amplitude of strain carry to early microcrack initiation, so from these growths of microcrack the lifetime of components is determined. The superimposed high cycle fatigue loading with amplitude of small strain under endurance limit for the relevant materials also minimize lifetime remarkably. Through this approach, we analyzed the superimposed HCF loading effect on FCG. The effect of superimposed HCF loading and the elastic behavior of long crack has been well investigated

in the existing literature. But the effect of LCF and HCF loading for the microcrack growth has not well investigated under plastic deformation of the relevant material. The following model was proposed for such mechanism:

$$\frac{da}{dN}|_{block} = \frac{da}{dN}|_{total} + \sum_{blocl}\frac{da}{dN}|_{HCF} \tag{2.8}$$

$\frac{da}{dN}|_{block}$ is the total increment of crack growth, $\frac{da}{dN}|_{total}$ is the total peak to peak loading cycle and $\sum_{blocl}\frac{da}{dN}|_{HCF}$ is the sum of all high cycle fatigue during one low cycle fatigue loading.

One block of loading comprises one low cycle fatigue loading and the corresponding superimposed high cycle fatigue loading as show in fig 2.5.
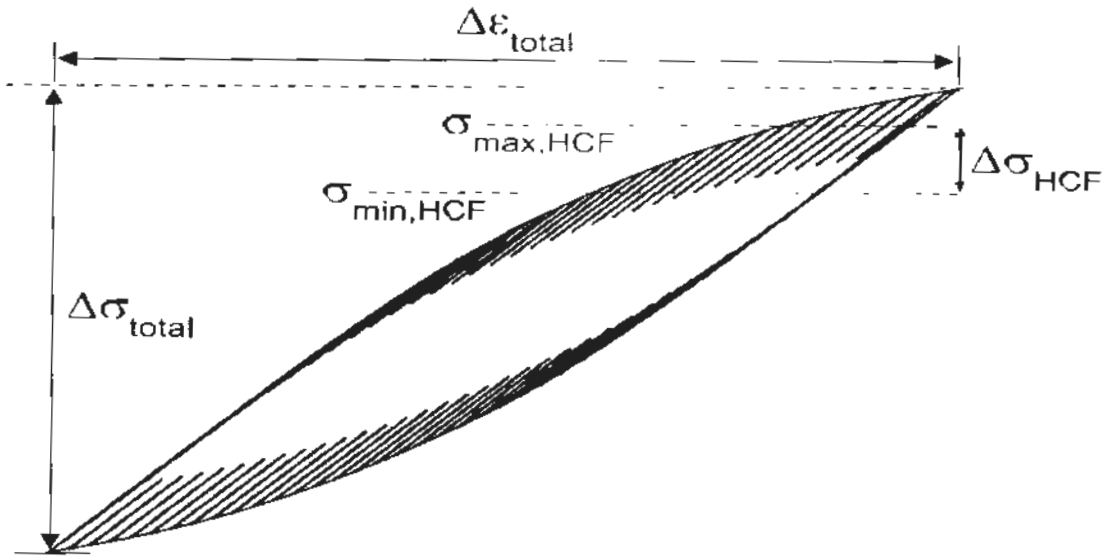
Figure 2.5: Schematic diagram of hysteresis loop for both LCF and HCF loading [17].

The above proposed model was presented to incorporate accelerated FCG rates under combine low and high cycle fatigue loadings. The model required few fitting parameters for validation. By using the linear correlation of crack growth and crack opening displacement range the proposed model narrate the crack length extension under low cycle fatigue loading, if period I FCG is not much prominent.

The above model was proposed to describe FCG curve under LCF and combine LCF/HCF loading but doesn't account TMF due to superimposed HCF loading [40]. The model was uniaxial and just incorporated LCF loading and combine LCF/HCF loading but was not extended to multiaxial loading as well as to HCF/TMF loading [17]. The model doesn't

consider the interaction effect of load which could influence strongly the stresses at the crack opening [41]. In the above approach, there was lack of numerical explanation about the interaction of HCF/LCF therefore not accurate for the validation of experimental data [42].

2.9 NASGRO Modified Model

Maierhofer, J. et. al [18] proposed NASGRO model to explain FCG mechanism for physically small crack. The theoretical analysis for FCG behavior under periodic loading at different stress range and with their respective stress intensity factor for any load ratio and crack extension is based on this equation. As we know that small crack is ability to grow beneath the threshold region for the growth of long crack, but small crack grows rapidly with respect to long crack under stress intensity factor of same domain. Generally used crack growth Model cannot describe the behaviour at all of short crack with good accuracy. There are so many types of small crack classified broadly in mechanically short crack, microstructurally short crack, chemically short crack and physically short crack. The purpose of this contribution is to develop a FCG model, which can describe the rate of crack growth for random length with the order of very small-scale yielding. The following supposition of crack growth analysis is based on the given mechanical Model in fig 2.6. Starting from a specimen having notch with depth of a_0 and a growing crack of length Δa are not subjected with a crack closure. Therefore, range of stress intensity factor is calculated by using the length of total crack but crack closure builds up occur may on the size of crack extension Δa only follow by the verification of NASGRO equation experimentally and then to remodel and take into account behaviour of small crack.
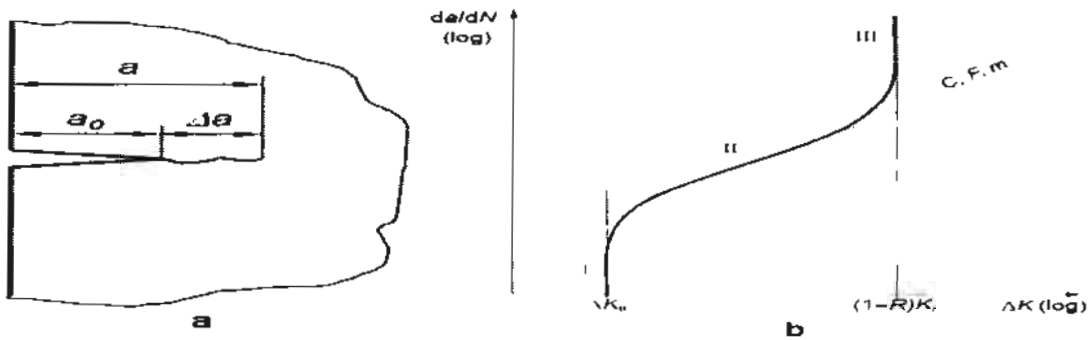

Figure 2.6: (a) Schematic diagram of mechanical model. (b) Typical long crack curve with constant load ratio [18].

$$\frac{da}{dN} = C.F \frac{(\Delta K - \Delta K_{th})^m}{1 - \frac{1}{1-R}\frac{\Delta K}{K_C}}$$ (2.9)

$\frac{da}{dN}$ represent crack growth rate, m and C arc constants experimentally estimated, F is the crack velocity factor, ΔK represent stress intensity factor range, ΔK_{th} represent threshold stress intensity factor range, R represent load ratio and K_C is the fracture toughness.

The above model represents all the branches of crack growth behavior. ΔK_{th} represent the position of branch I while the parameters C, m and F represents the position of branch II and K_C represent the position of transition from Paris state to unstable state of crack growth.

To adjust the model of NASGRO to the behavior of small crack will take into account the following points:

(1) That small crack will grow for long crack below the threshold.

(2) That small crack grows rapidly with respect to long crack for same stress intensity factor rang mostly in the region of low and medium threshold regime like Paris region.

So, it is found from the above model that crack closure effect is increasing with crack extension and also the modified NASGRO model can estimate the growth rate of crack length randomly. This approach is good with respect to other to calculate the life time accurately.

The above model analyses the behaviour of small crack experimentally well but the contribution of roughness induce and plasticity induce crack closure show the difference between materials which doesn't comparable to one another. As the crack closure mechanism show difference as a result threshold limit of long crack show variation. NASGRO modified model ignored these points in his model [43].

2.10 Shan Jiang Model

Shan Jiang et al [19] proposed an analytical model to predict FCG behavior under a single overload with constant amplitude. In this model for by using plastic zone and crack closure was accounted crack growth retardation. The virtual crack annealing modified model by Bauschinger effect was used to compute the range of crack closure outside the region of retardation effect. And the plastic zone model of Dugdale was used to estimate retardation effect region size. A sophisticated mathematical equation was developed to estimate the variation in crack closure during retardation area.

$$\frac{da}{dN} = C(\Delta K_{eff})^m \tag{2.10}$$

$\Delta K_{eff=K_{max}-K_{op}}$

$\frac{da}{dN}$ is the crack growth rate, ΔK_{eff} represent stress intensity factor range, C as well m are the empirical parameters, K_{max} represent maximum stress intensity factor and K_{op} represent crack closure level.

The above analytical model was derived from FCG mechanisms like crack closure, Bauschinger effect and plastic zone and doesn't required any extra parameters which have no physical meaning. The above model is only valid for the current loading spectrum and materials. But in future the present frame work of this model will be extended to other materials.

The above model doesn't explain bifurcation and branching due to overload which can retard the growth rate of crack. Also, the model was suitable only for the present investigated materials and loading spectrum [19].

CHAPTER 3

MECHANISTIC MODEL DEVELOPMENT

In this chapter, an analytical model for fatigue crack growth is developed based on two fracture mechanics parameters. The fractographic features of the crack growth will be used for the development of the model. First of all, we will describe the mechanism of striation formation. Then it will be followed by the sections which will describe the influence of ΔK and stress ratio on the fatigue striations the influence of ΔK and stress ratio on FCG and then analytical model will be described.

3.1 Mechanism of striation formation

The most important fractographic features of the fatigue fracture is striation [44]. The mechanism of striation formation has been explaining by many models. The oldest and popular model about striation was proposed by Laird's Model [45,46]. He examines the specimen of metal ductile broken under high fatigue stress which appear like the fracture ripple on the fracture surface similar to the resulting from low fatigue stress but normally larger. It has been observed that fracture ripple formation and crack propagation are due to re-sharping and blunting of crack-tip on every cycle of stress. Francois et al [47] describing the mechanism of fatigue striation in Fig 3.1 how to form the first striation when the crack passes from region I to region II of propagation. During unloading the shape of crack tip is sharp but when the load is increased the shape of crack-tip become blunt and thus the process is going on as a result striation is generated after one complete stress cycle.
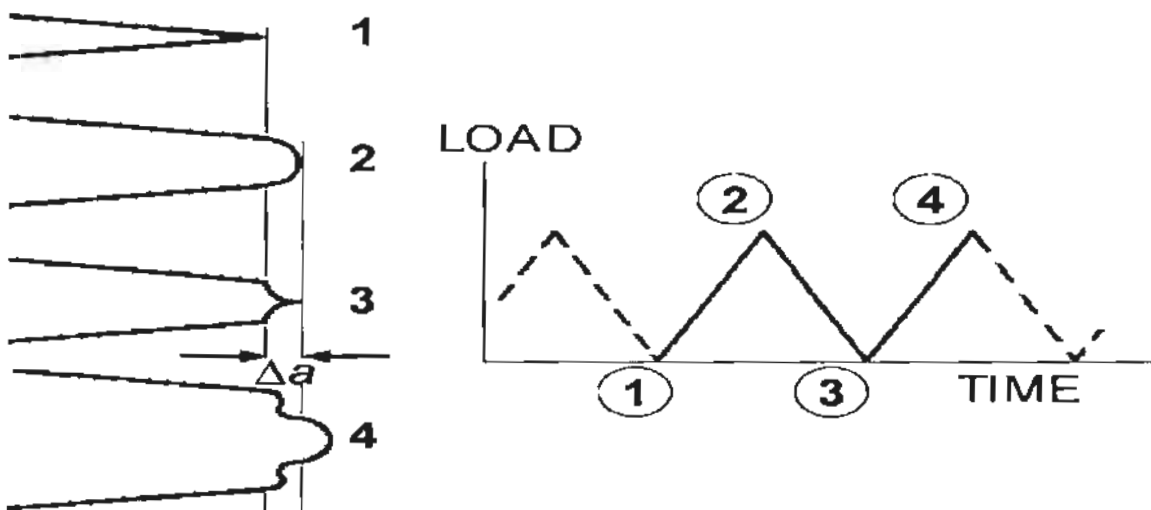

Figure 3.1: Striation formation mechanism [47]

Milella et al [48] described the formation of striation that it is the microscopic feature left on the fracture surface which identify the FCG. Striation is generated at the tip of crack due micro-plasticity. Plastic blunting during loading and re-sharping during unloading lead the formation of striation as shown in Fig 3.2.
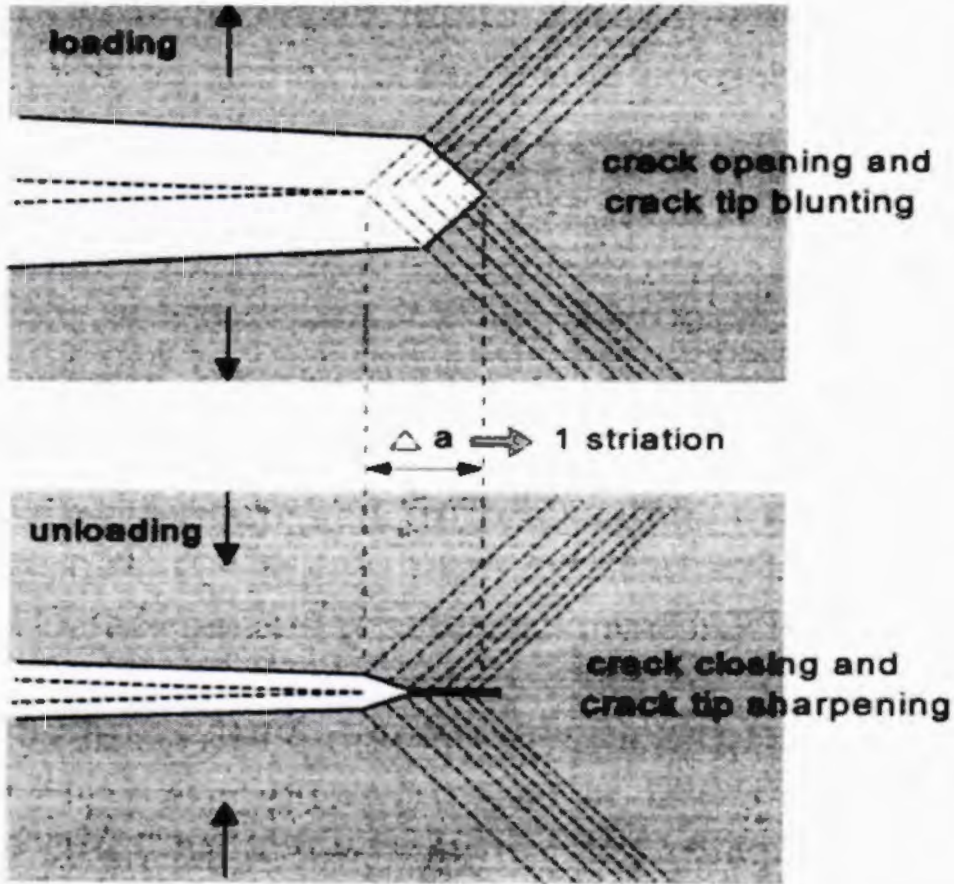

Figure 3.2: Crack tip blunting and re-sharping mechanism [48]

Some authors proposed different models that the striation spacing is equal to the macroscopic crack growth rate ($v = s$) but this equivalence is valid only for a limited range of ΔK [49, 50, 51]. There are some cases for which ($v = s$) but generally striation spacing show deviation from macroscopic crack growth rate [8, 52, 53].

3.2 Influence of ΔK and stress ratio on fatigue striation

Benachour et al [54] investigated that ΔK and mean stress or stress ratio both have the similar effects on the striation spacing i.e. Striation spacing increases with both ΔK and mean stress. At constant amplitude of loading during propagation for different load ratio the striations were observed. It can be seen for the crack growth of same length after the fracture surface of final failure that the load ratio increases fatigue striation spacing as shown in Fig 3.3.
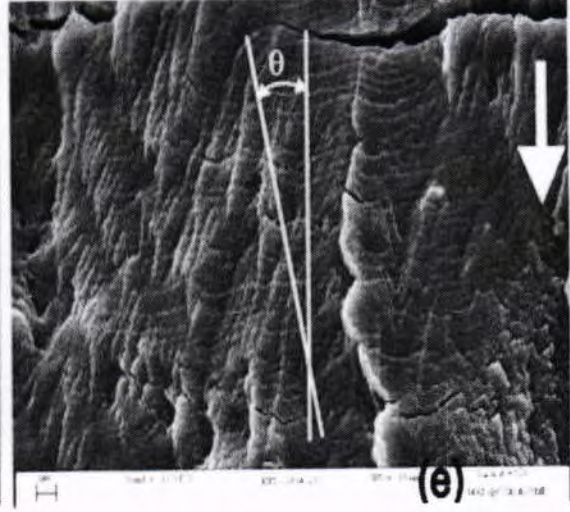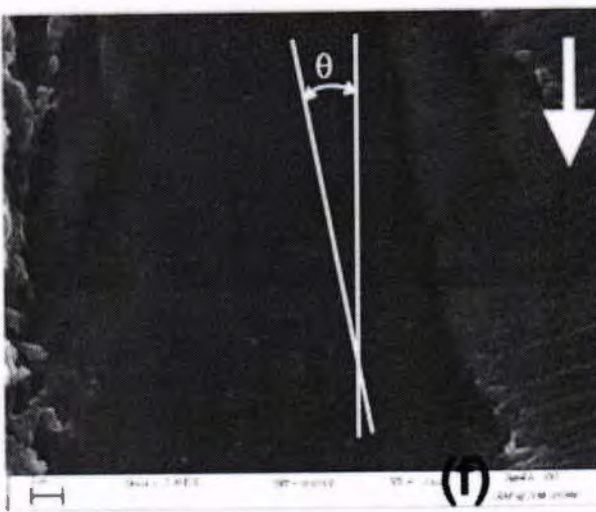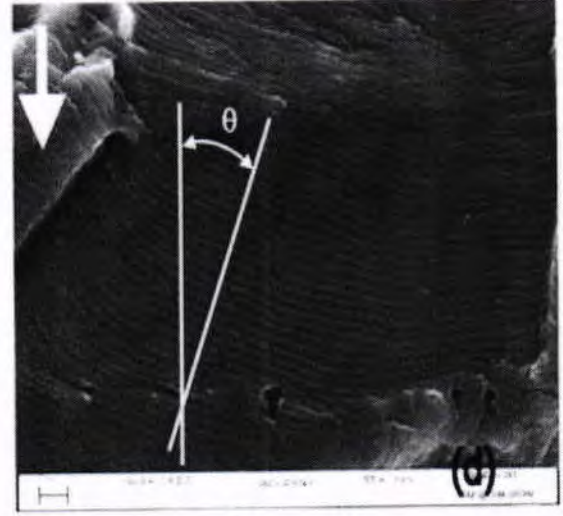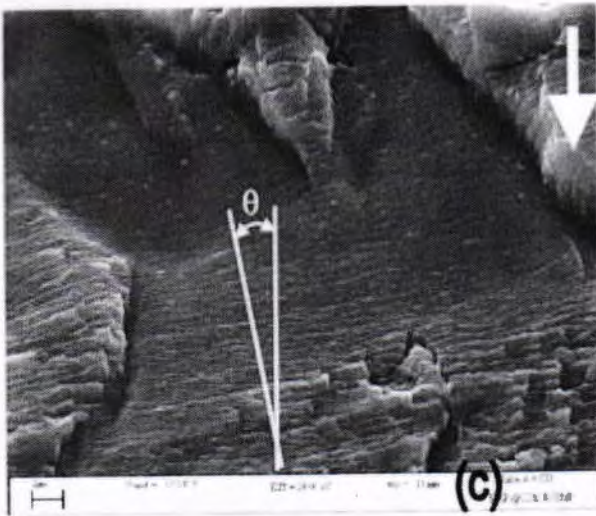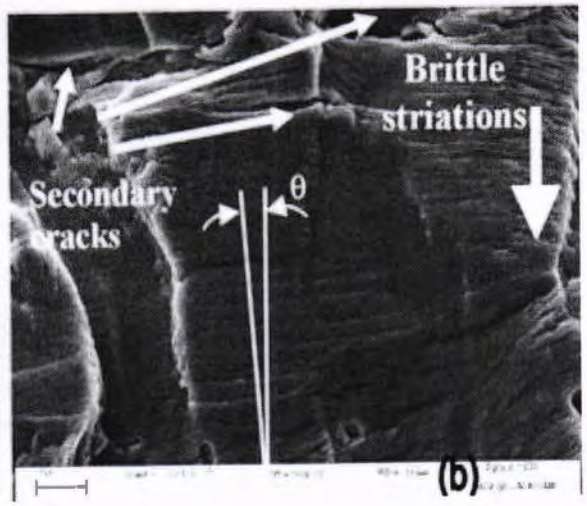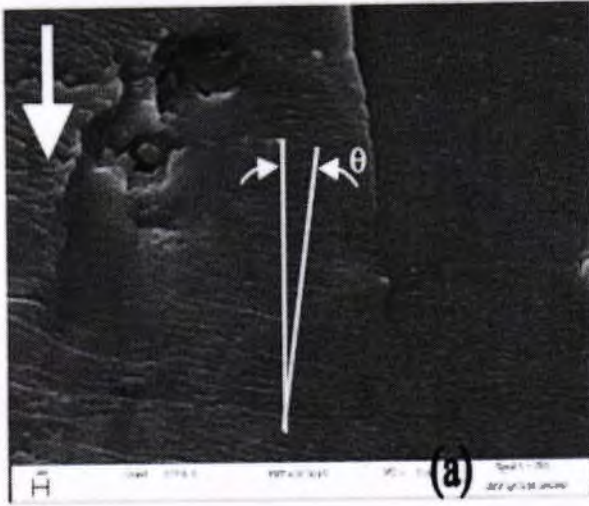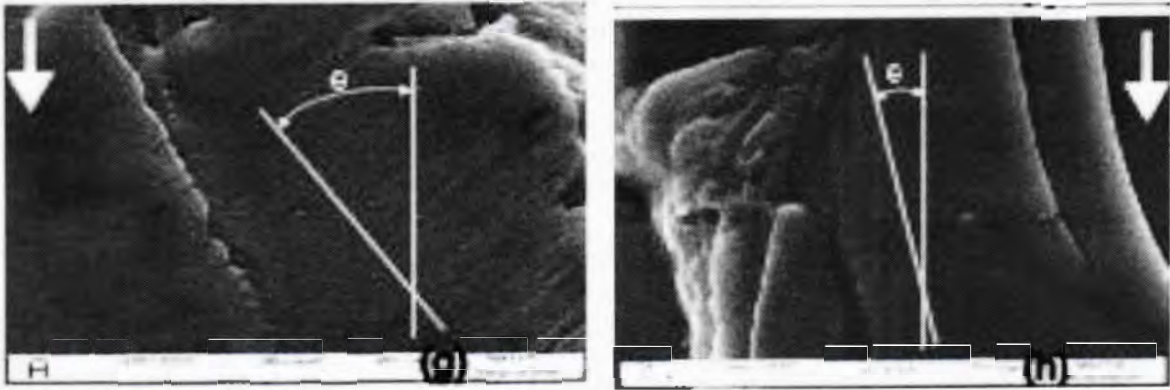
Figure 3.3: Fatigue striation spacing at different load ratio [54]

The above fracture surface show that the striation spacing increases with increases the stress ratios as shown in Table 3.1. Also, it was investigated that fracture surface observation show us that striations are normal to direction inclined with an angle to the propagation direction. The above Fig 3.3 also shows us the influence of stress ratio with the relevant angle. The angle show variation on different stress ratios.

Table 3.1 Striation spacing at different stress ratios [54]

Sr No	Stress Ratio	Crack size	Striation spacing $(\frac{da}{dN})$
a	0.1	5.95mm	4.28×10-4mm/cycle
b	0.1	7.24mm	3.23×10-3mm/cycle
c	0.2	5.89mm	4.0×10-4 mm/cycle
d	0.2	7.00mm	5.6×10-3 mm/cycle
e	0.3	5.71mm	5.83×10-4mm/cycle
f	0.3	7.67mm	3.33×10-4mm/cycle
g	0.5	5.81mm	1.25×10-3mm/cycle
h	0.5	6.00mm	1.28×10-3mm/cycle

It was investigated that the slope of striations spacing is different from the macroscopic FCG slope at small stress ratio (R=0.1, 0.2, 0,3) but the slope converges on (R=0.5) to the macroscopic FCG rates slope as shown in table 3.2.

Table 3.2: Paris Law parameters in function of stress ratio [54]

Stress ratio	C (mm/cycle)	M
0.1	2×10^{-9}	4.294
0.2	2×10^{-9}	4.447
0.3	2×10^{-8}	3.450
0.5	8×10^{-8}	2.834

Micro FCG rates (Fatigue striation spacing) are plotted for all stress ratio as shown in Fig 3.4.
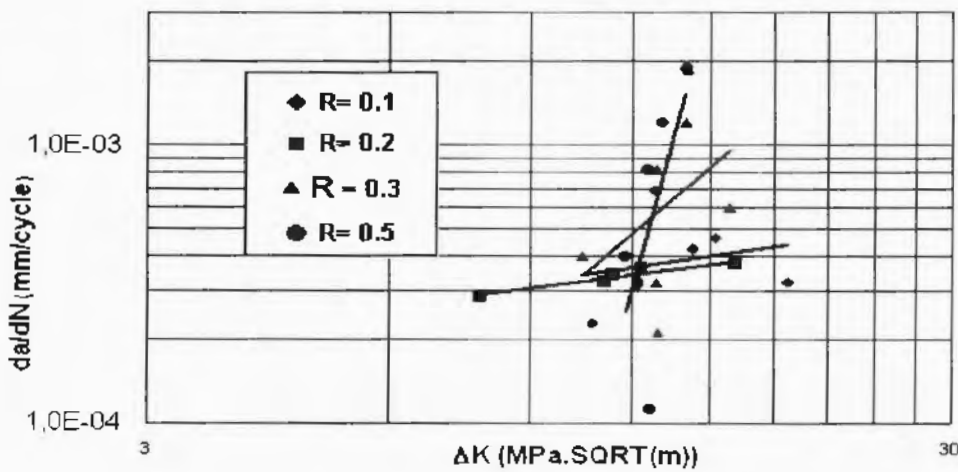
Figure 3.4: Striation spacing at different load ratio [54]

The above graph in fig 3.4 show us that when the effect of stress ratio increases at the same the fatigue striation spacing also increases for the given value of ΔK. Also, the graph shows us the effect of stress ratio on fatigue striation.

3.3 Effects of stress ratio and ΔK on FCG rates

Furukawa [55] has developed a new approach for the determination of service load from fatigue striation spacing during the investigation of fatigue crack growth of 2017 T4 alloy of Aluminum. The relationship between fatigue striation spacing and the range of stress intensity factor show that the fatigue crack growth rates is only not influence by ΔK but influence also by load ratio. E.U. Lee et al [56] show the variation of FCG rates versus ΔK in Fig 3.5 at

23

different load ratios in different environments. While increasing the stress ratio will also increase the fatigue crack growth rate.
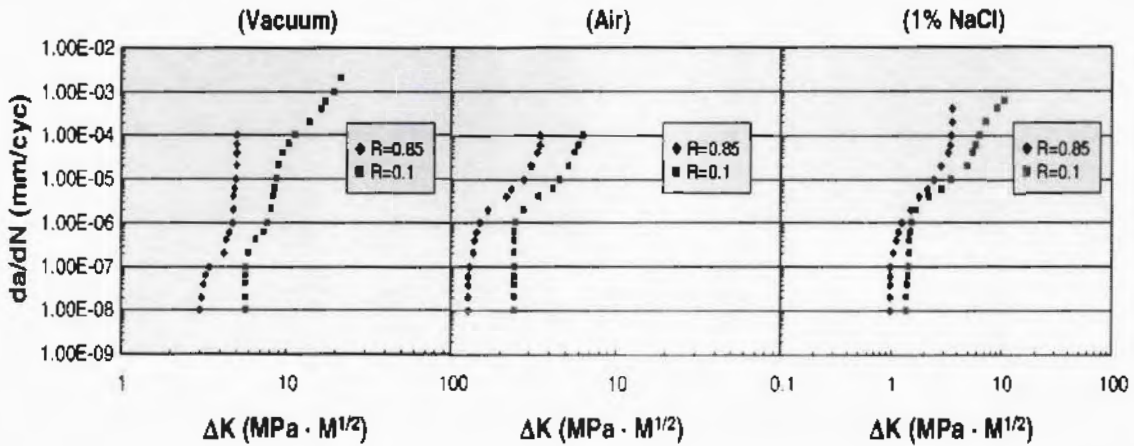
Figure 3.5: FCG rates versus ΔK [56].

It is found by Benachour et al [54] that Paris region satisfy $\frac{da}{dN}$, ΔK and striation spacing in its experiment.

3.4 Model development

From the above section, we can conclude that FCG rate are the function of two parameters ΔK and stress ratio or mean stress. Various models were developed to accounts for the effect of stress ratios and ΔK for the crack growth. The famous model proposed by Forman et al [57] incorporated these two parameters in the model but didn't describe the physical mechanism because the model was empirical based. Benachour et al [54] predict that by increases stress ratio will increased the plastic zone size for the given value of ΔK. If we keep ΔK constant and increase the stress ratio will also increase the plastic zone. Magnus Hörnqvist et al [58] describe that if we keep ΔK constant the fatigue crack growth show variation with corresponding stress ratio.
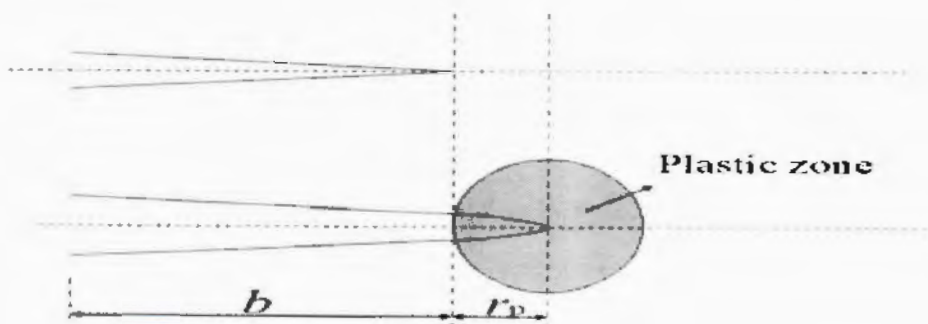
Figure 3.6: Plastic zone size formation mechanism [16]

24

In the above diagram b represent the depth of initial crack and r_p represent the plastic zone radius at the crack-tip. The above diagram show us that bluntness will be the function of local material plasticity [16].

If the stress ratio increases for the given value of ΔK thus the plastic zone also increases as show schematically in the following way.

In the following case, we assume that $R_2 > R_1$

Fig 3.7: Schematically plastic zone sizes at R_1 and R_2

It means as the effect of stress ratio increases as a result the plastic zone size will increase thus the striation spacing will increases.

As FCG rates is the function of two parameters according to the above discussion so we can write it in the following form:

$$\frac{da}{dN} = f(\Delta K, \ K_{mean})$$ (3.1)

Where $\Delta K = K_{max} - K_{min}$, and $K_{mean} = \frac{K_{min} + K_{max}}{2}$

By using the principle of superposition [59] rewrite equation (3.1) in the following way:

$$\frac{da}{dN} = A(\Delta K)^m + B(K_{mean})^n$$ (3.2)

A, B, m and n are equation parameters determined experimentally

Fatigue phenomenon can be described by any of the following five parameters.

K_{max}, K_{min}, K_{mean}, ΔK and R

The above model given by equation (3.2) contains two parameters so this implies that fatigue crack growth is also the function of two parameters. For the fatigue spectrum, at least

25

two parameters are needed. This implies that the crack growth rate should be also described by any of two parameters.

Fatigue crack growth is affected by both types of loading cyclic as well as monotonic loading. The effect of monotonic loading is known as stress ratio effect.

Based upon fractographical analysis, a two-parameter model has been developed in which the contribution of cyclic loading and monotonic loading superimposed rather than multiplied. The above two-parameters model will be validated in the next cbapter with authentic experimental data.

CHAPTER 4

MODEL IMPLEMENTATION AND VALIDATION

In this chapter, the model developed in the previous chapter has been implemented and validated by using open source literature experimental data in the fatigue crack growth. Four case studies are discussed in this chapter.

4.1 Case study I:

The first data set was taken from the work of Chang et al [60]. The material used in their study was 300M steel. The material was tested at different stress ratios. The fatigue crack growth data at stress ratios R=0.7, R=0.5 and R=0.3 is used for the implementation of the current model:

$$\frac{da}{dN} = A(\Delta K)^m + B(K_{mean})^n \tag{4.1}$$

The test data at stress ratio R=0.05 is used for the validation of the above model. The experimental data for the stress ratios 0.7,0.5 and 0.3 is plotted in 3D plot as shown in the figure 4.1.

Figure 4.1: Crack growth data $\frac{da}{dN}$ verses ΔK and K_{mean} [60]

The model parameters were obtained by using surface fitting tool of MATLAB. After several trials, the values of the model parameters were chosen for the highest R^2, equal to 0.9606.

The model parameters were as under.

A= $5.437e^{-08}$, m=2.22

B=$1.7408e^{-08}$, n=2

The surface fitting to the experimental data is shown in 3D plot of $\frac{da}{dN}$ verses ΔK and K_{mean} in figure 4.2.

The final model is given by equation 4.2.

$$\frac{da}{dN} = 5.437e^{-08}\Delta K^{2.22} + 1.7408e^{-08}K_{mean}{}^2 \qquad (4.2)$$
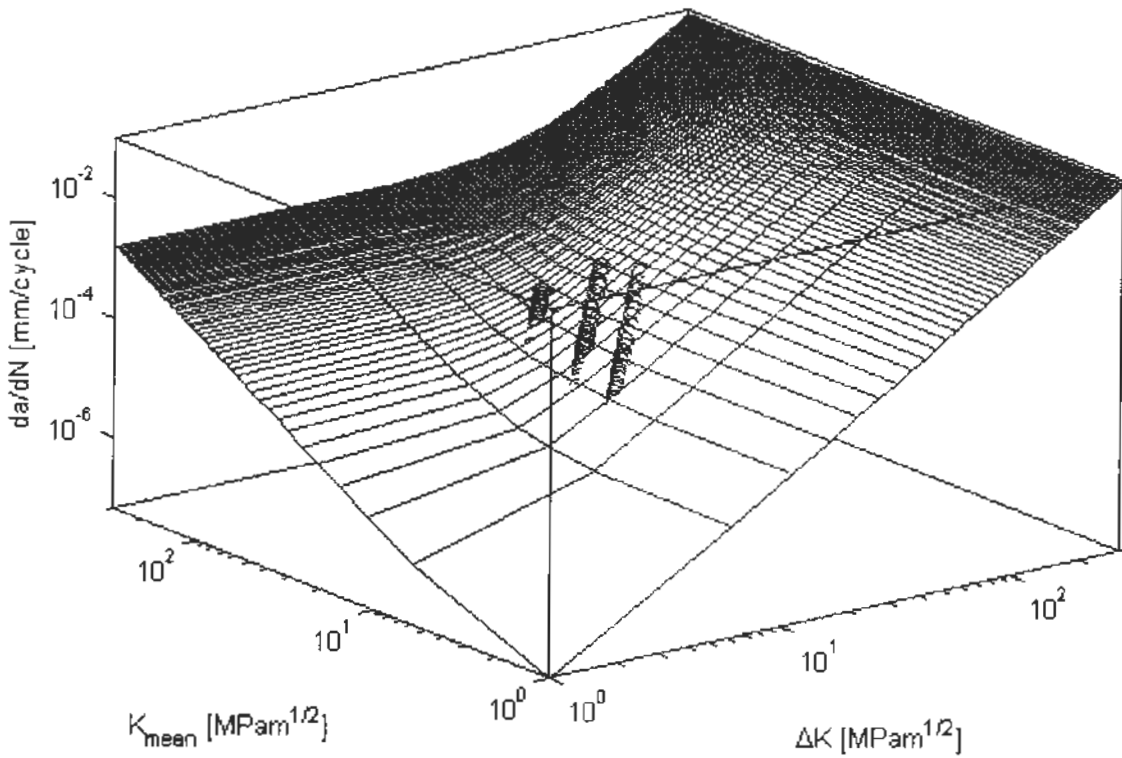
Figure 4.2: Surface fitting to the data in figure 4.1

For the current model validation, the equation 4.2 is transformed to single variable in term of ΔK as given in equation 4.3:

$$\frac{da}{dN} = 5.437e^{-08}\Delta K^{2.22} + 6.61e^{-08}\Delta K^2 \qquad (4.3)$$
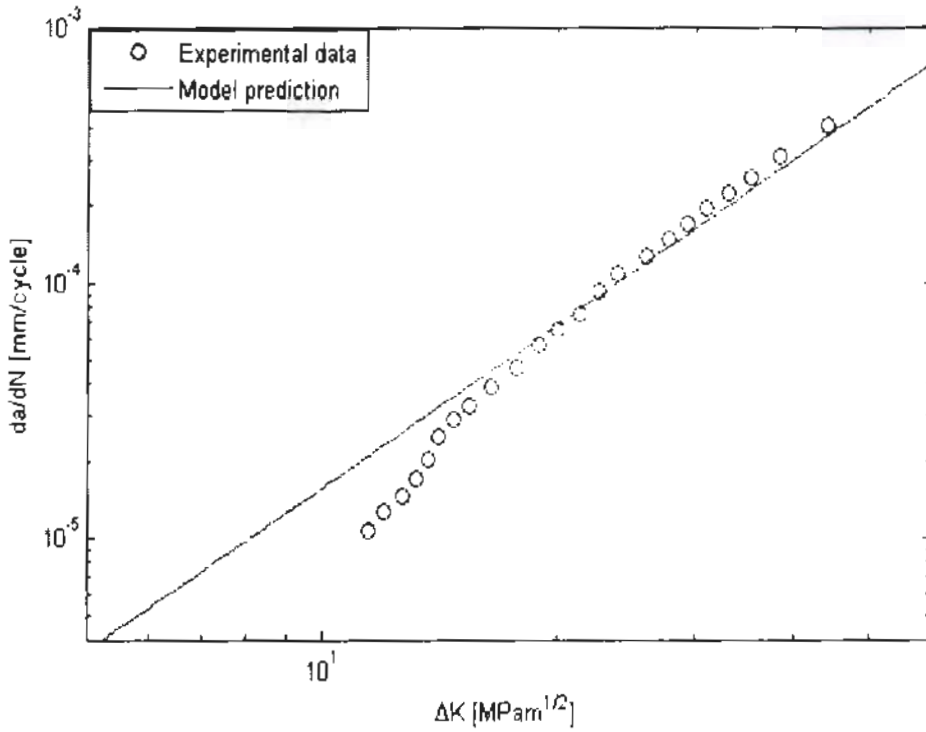
Figure 4.3: Model validation of case study I.

Figure 4.3 shows 2D plot of $\frac{da}{dN}$ versus ΔK to check the performance of the model validation. The figure shows a good relationship between experimental data and model prediction in the linear region. However, at lower ΔK the deviation of the experimental data from model prediction is seen. The model prediction is slightly higher than the experimental data as show in figure 4.3.

4.2 Case study II:

The second data set was taken from the work of Tsudka [61]. The material was medium carbon structural steel. Four stress ratios were used for the implementation of the current model as shown in equation 4.4 are R= 0.5, R= 0.4, R=0.3 and R=0.0.

$$\frac{da}{dN} = A(\Delta K)^m + B(K_{mean})^n \tag{4.4}$$

But the test data at stress ratio 0.05 is used for the validation of the above model. The experimental data for the stress ratios R= 0.5, R= 0.4, R=0.3 and R=0.0 is plotted in 3D form as shown in the figure 4.4.
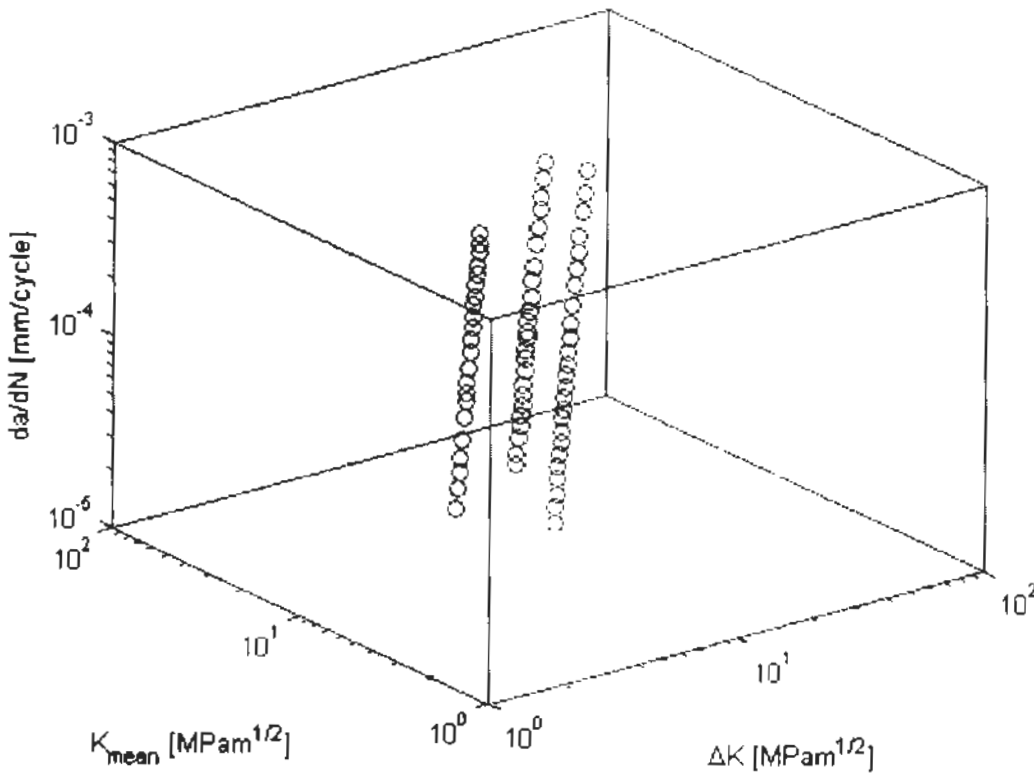
Figure 4.4: Crack growth data $\frac{da}{dN}$ verses ΔK and K_{mean} [61]

By using surface fitting tool of MATLAB parameters for the current model obtained. After several time trials in curve fitting tool of MATLAB the values of the model parameters were obtained for the highest R^2, equal to 0.9546.

The model parameters were as under.

A= $1.899e^{-11}$, m=2.5

B=$1.31e^{-11}$, n=1.2

The surface fitting to the experimental data as shown in 3D plot of $\frac{da}{dN}$ verses ΔK and K_{mean} in figure 4.5.
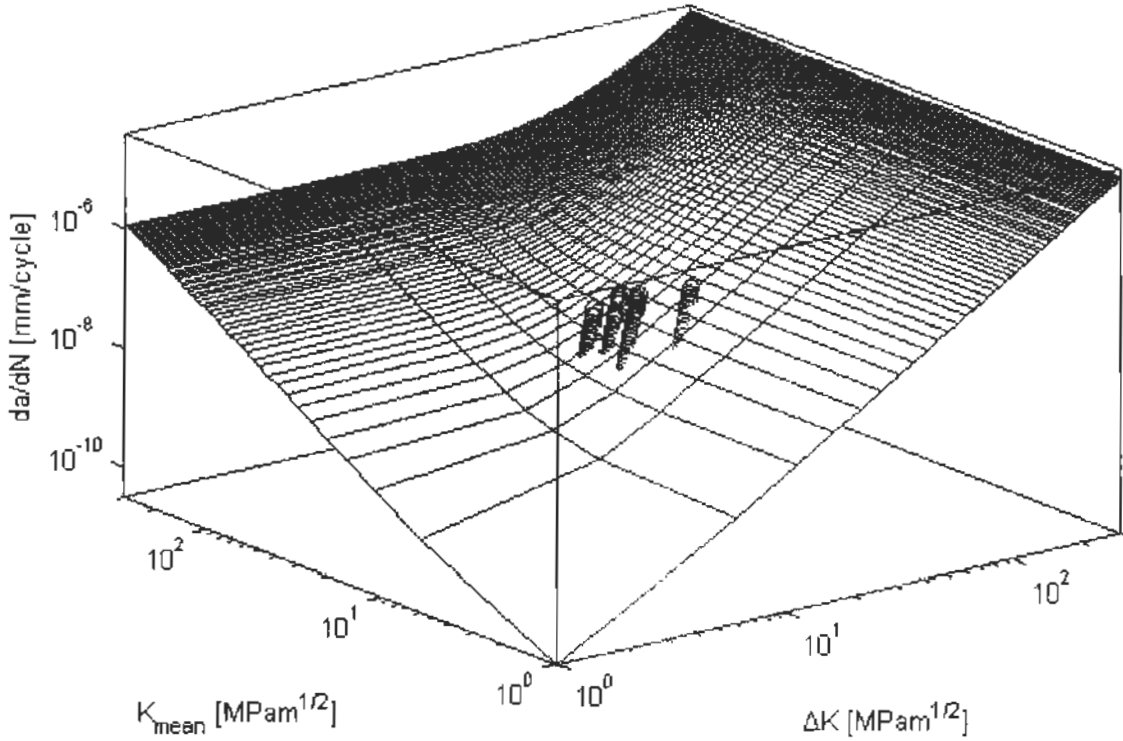
Figure 4.5: Surface fitting to the data in figure 4.4

The shape of the model for the current parameters as given by equation 4.5:

$$\frac{da}{dN} = 1.899e^{-11}\Delta K^{2.5} + 1.31e^{-11}\text{K}_{\text{mean}}{}^{1.2} \tag{4.5}$$

For the validation of the current model the above equation 4.5 is transformed into single variable in term of ΔK as given by the following equation:

$$\frac{da}{dN} = 1.899e^{-11}\Delta K^{2.5} + 1.051e^{-10}\Delta K^{1.2} \tag{4.6}$$

Figure 4.6 shows us the 2D form of the $\frac{da}{dN}$ verses ΔK for checking the performance of model validation.

31
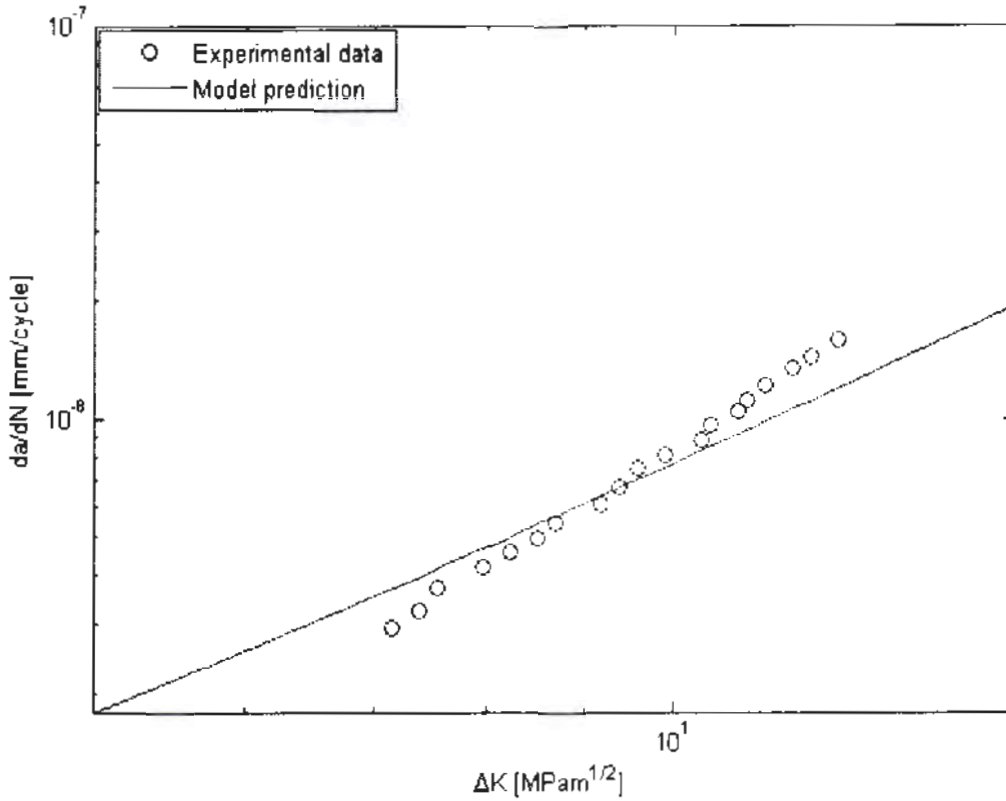
Figure 4.6: Model validation of case study II.

The above figure shows a good correlation between the experimental data and the model prediction in the Paris region. At lower value of ΔK experimental data is lower than model prediction but as the value of ΔK increases the experimental value become higher than the model prediction as shown in the above figure 4.6.

4.3 Case study III

The data set used in this case was taken from the work of Dubey [62]. The material used in their experiment was Ti–6Al–4V. During performing his experiment on the given material, they used various stress ratios. The data of fatigue crack growth at stress ratios R=0.8, R=0.5 and R=0.25 is used for the implementation of the following model:

$$\frac{da}{dN} = A(\Delta K)^m + B(K_{mean})^n \tag{4.7}$$

But the remaining test data at stress ratio R=0.02 is used for the validation of above model. The experimental data at the stress ratios R=0.8, R=0.5 and R=0.25 is plotted in 3D plot form as shown in the figure 4.7.

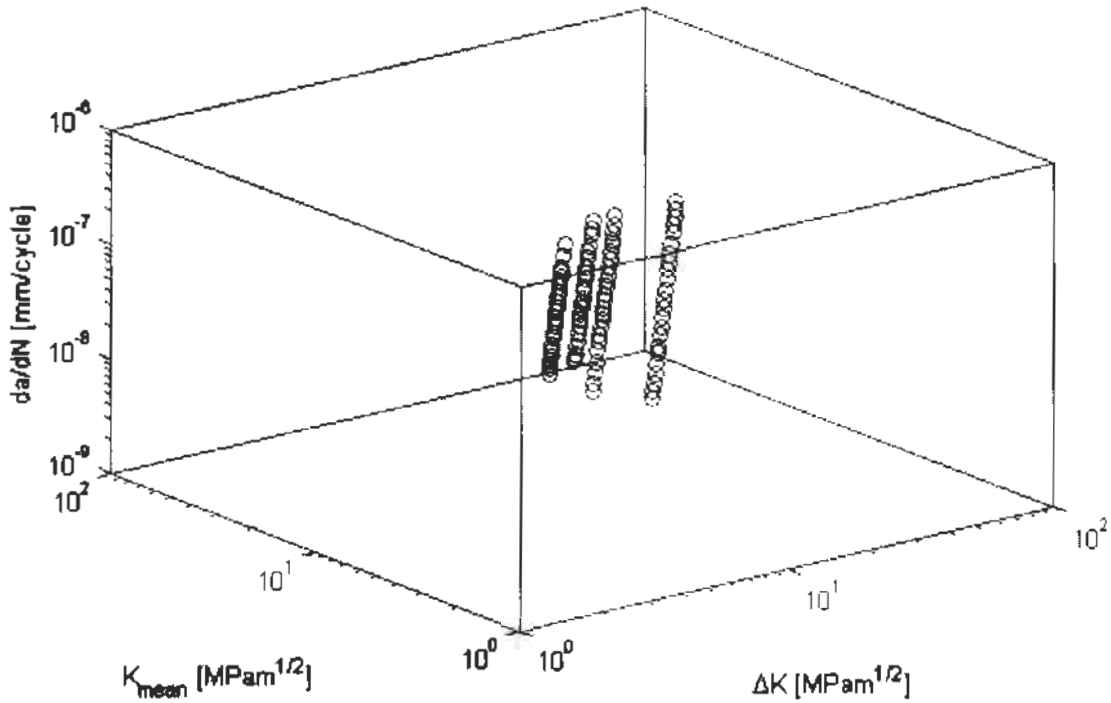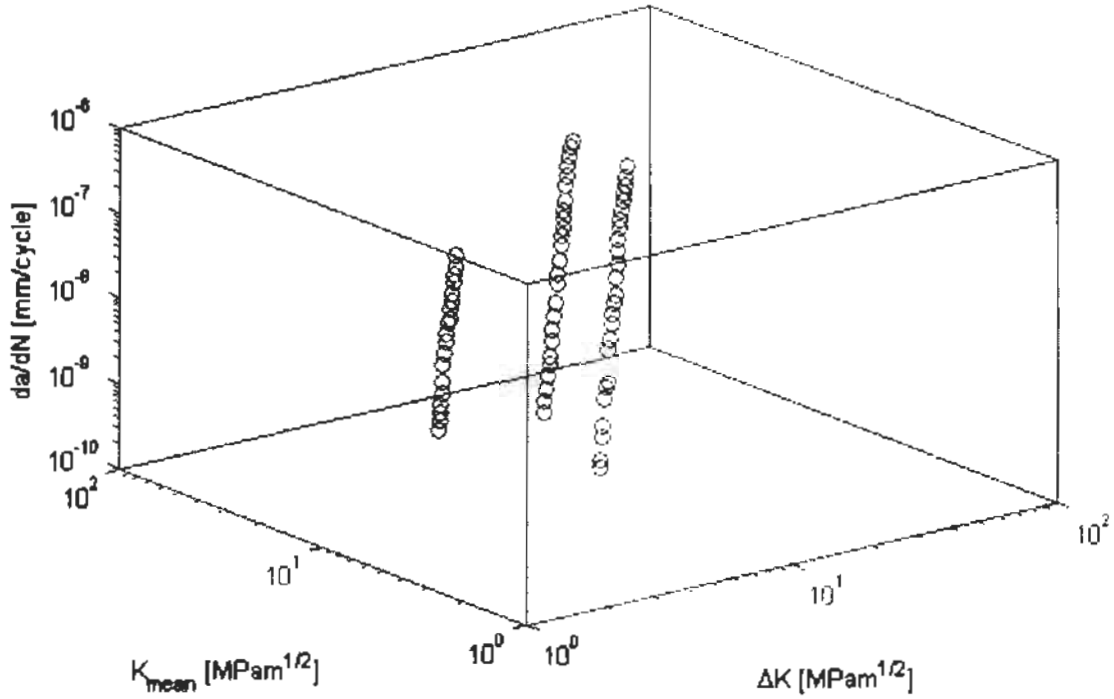**Figure 4.7:** Crack growth data $\frac{da}{dN}$ verses ΔK and K_{mean} [62]

The model parameters were obtained with the help of surface fitting tool of MATLAB. By doing several trials in surface fitting tool the values of the model parameters were chosen at the highest value of R^2, which was equal to 0.7263.

The model parameters were as under.

A= $3.221e^{-12}$, m=2.4

B=$8.963e^{-12}$, n=2.66

According to the above model parameters the following shape of the model is made:

$$\frac{da}{dN} = 3.221e^{-12}\Delta K^{2.4} + 8.963e^{-12}K_{mean}{}^{2.66} \qquad (4.8)$$

For the current case, the surface fitting to the experimental data as shown in the 3D plot form of $\frac{da}{dN}$ verses ΔK and K_{mean} in figure 4.8.

Figure 4.8: Surface fitting to the data in figure 4.7

For the validation of the current model equation 4.8 is transformed into single variable form in term of ΔK as given by equation 4.9:

$$\frac{da}{dN} = 3.221e^{-12}\Delta K^{2.4} + 4.666e^{-11}\Delta K^{2.66} \tag{4.9}$$

To check the performance of the current model validation from the figure 4.9 in 2D form of $\frac{da}{dN}$ verses ΔK. The figure 4.9 shows a weak relationship between experimental data and model prediction. At lower value of ΔK the experimental data is lower than model prediction. The sensitivity of the model prediction is significantly lower than the experimental data as show in figure 4.9.
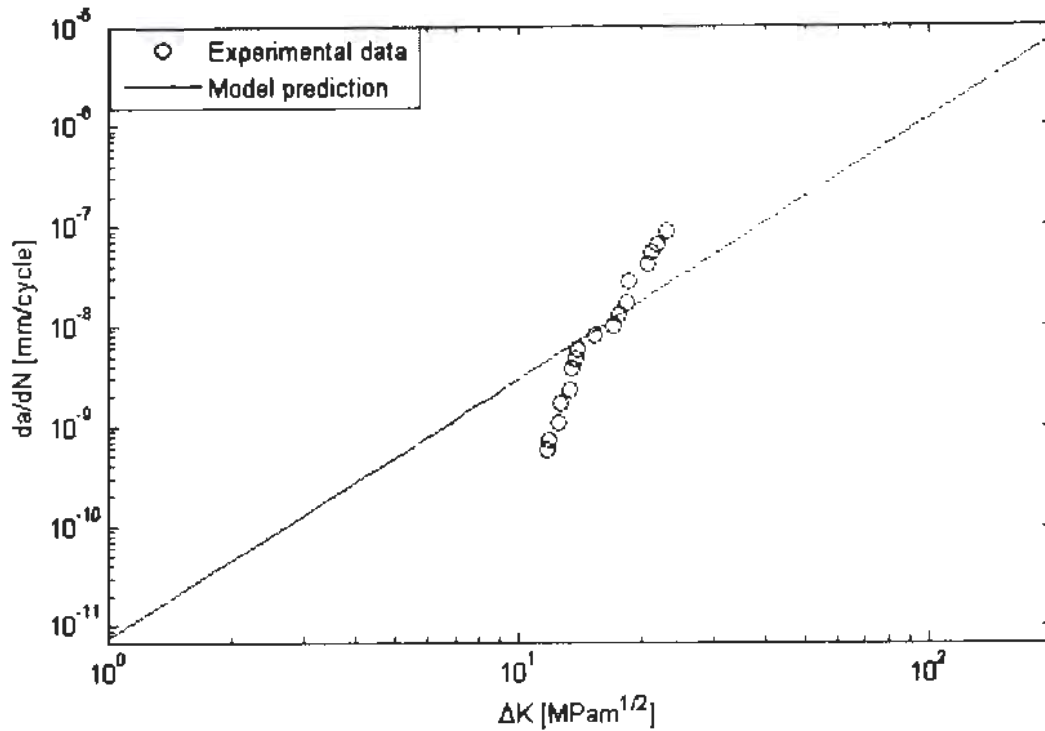
Figure 4.9: Model validation of case study III.

4.4 Case study VI

The experimental data for this case has been taken from the work done by Paris [9].They used material 6013-T651 aluminum alloy during in its experiment. For the implementation of the current model as given in equation 4.10 the fatigue crack growth data at stress ratios R=-1, R=0.10, R=0.30 and R=0.50 are used.

$$\frac{da}{dN} = A(\Delta K)^m + B(K_{mean})^n \qquad (4.10)$$

The above model was validated using test data at stress ratio 0.70. Experimental data for the current case is plotted in 3D form for the stress ratios R=-1, R=0.10, R=0.30 and R=0.50 as shown in figure 4.10.
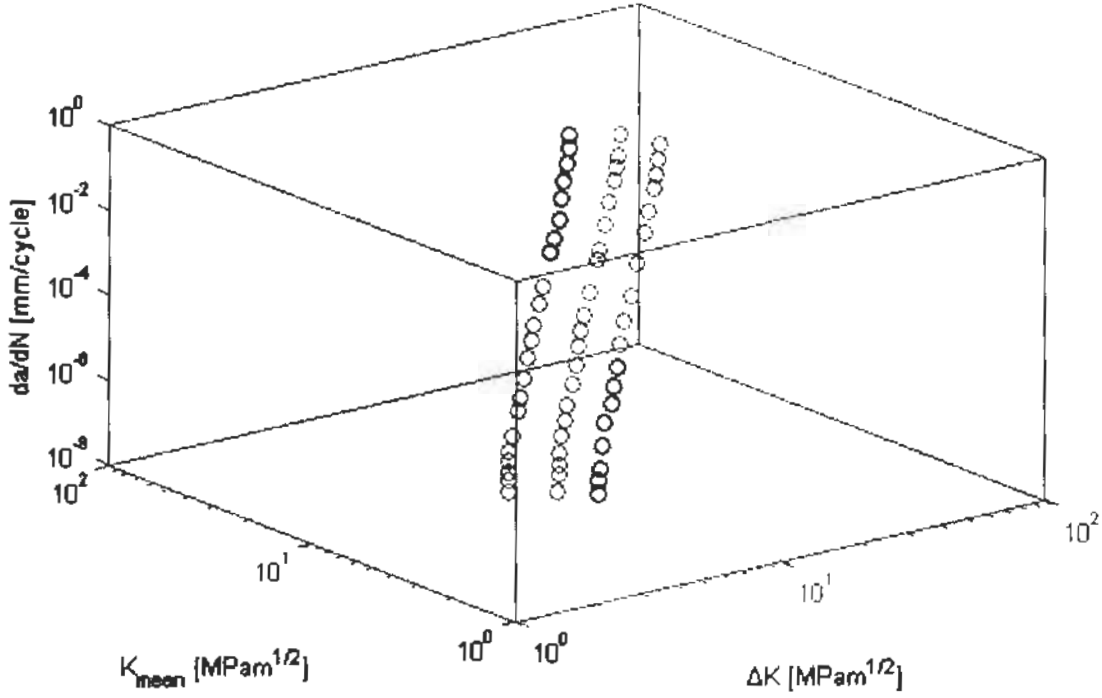
Figure 4.10: Crack growth data $\frac{da}{dN}$ verses ΔK and K_{mean} [9]

The model parameters were obtained by using same technique as for previous cases. After several trials, the values of the model parameters were chosen for the highest value of R^2, equal to 0.9428.

The model parameters were as under.

A= $2.452e^{-07}$, m=2.5

B=$2.293e^{-07}$, n=3.33

The final model shape for the current parameters is given by equation 4.11

$$\frac{da}{dN} = 2.452e^{-07}\Delta K^{2.5} + 2.293e^{-07}K_{mean}^{\,3.33} \tag{4.11}$$

The surface fitting to the experimental data is shown in 3D plot of $\frac{da}{dN}$ verses ΔK and K_{mean} in figure 4.11.

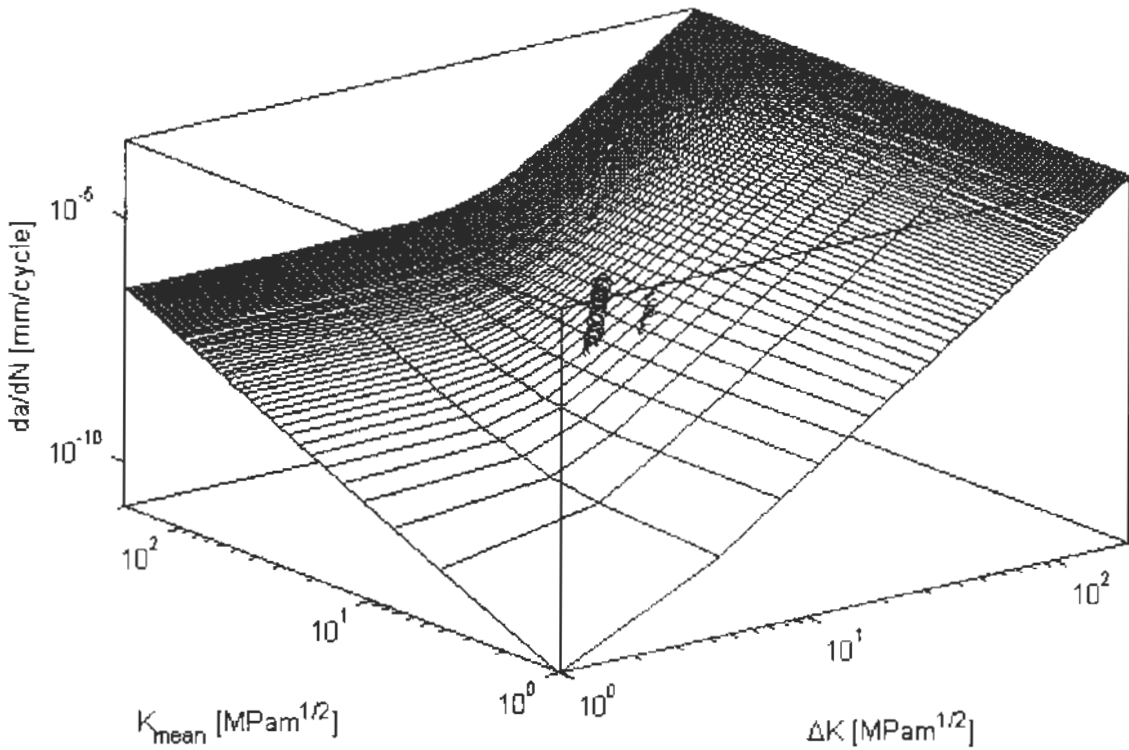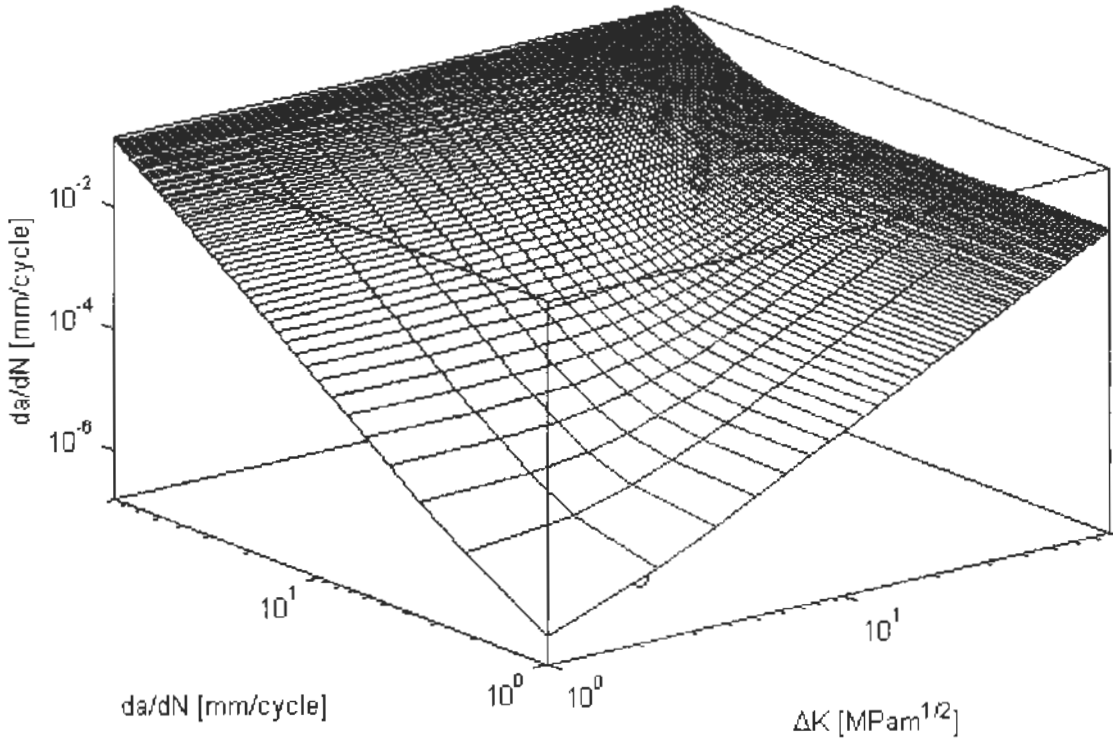**Figure 4.11:** Surface fitting to the data in figure 4.10

For the model validation equation 4.11 is transformed into one variable form in term of ΔK as given by equation 4.12.

$$\frac{da}{dN} = 2.452e^{-07}\Delta K^{2.5} + 5.2155e^{-08}\Delta K^{3.33} \tag{4.12}$$

Figure 4.12 shows 2D plot of $\frac{da}{dN}$ verses ΔK to check the performance of model validation. The figure shows a good relationship between the experimental data and the model prediction in the Paris region. But still there is some deviation of experimental data from model prediction as shown in the figure 4.12. At the early stage, the experimental data is lower than model prediction. This shows that in region II prediction is good, however in threshold region the model prediction deviates from test data.
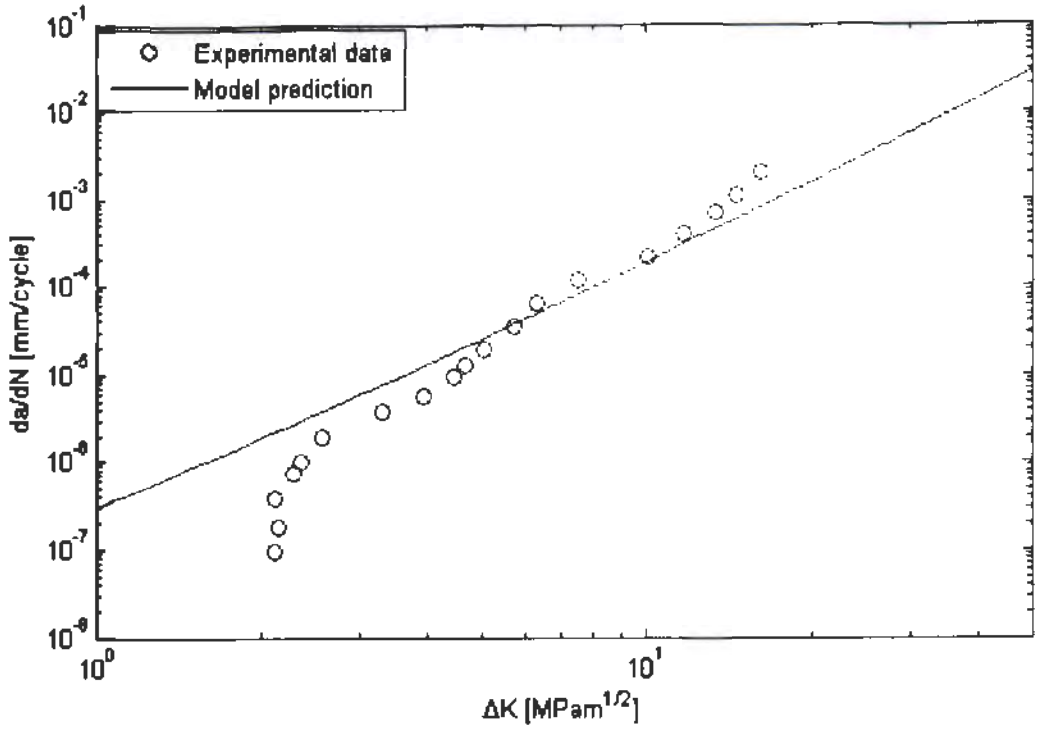
Figure 4.12: Model validation of case study IV.

CHAPTER 5

DISCUSSION

In this chapter, the modelling of Fatigue crack growth has been discussed in contest with major parameters and that play role in its characterization with reference to the current research. Section 5.1 discussed Fatigue crack growth regions according to applied loading values, section 5.2 discusses the fracture feature contribution in the modelling and section 5.3 discusses use of similitude parameters in Fatigue crack growth models.

5.1 Fatigue crack growth regions

According to the applied stress intensity factor range ΔK, the FCG curve has sigmoidal shape as shown in figure 5.1. FCG curve can be divided in three regions according to the slope variation in this curve. These regions are often termed as region I, region II and region III. These regions basically show the sensitivity of the Fatigue crack growth rate to the SIF range.
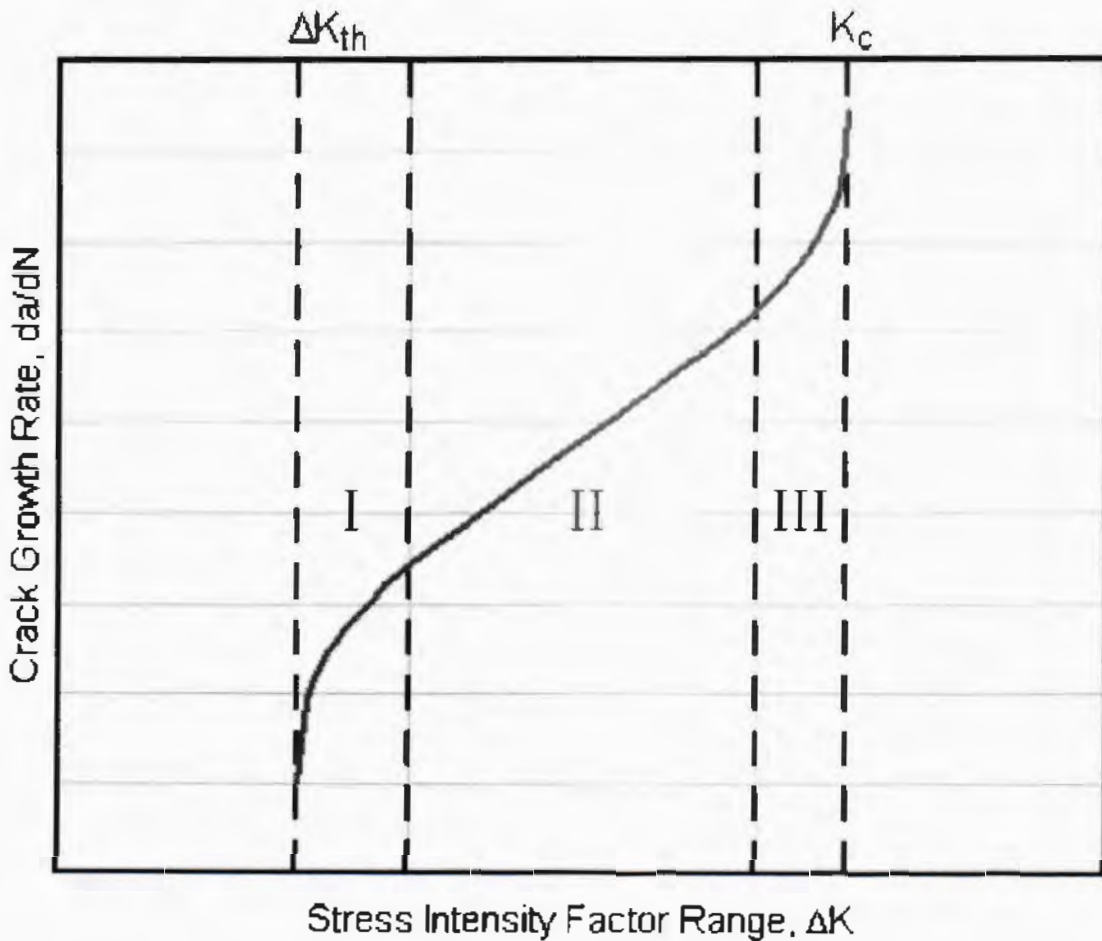
Figure 5.1: FCG rates verses ΔK [63]

5.1.1 Region I

In region I, the growth rate is more sensitive to the ΔK. The slope of curve is sharp which implies that small variation in ΔK bring large variation in the FCG. In this region, the effect of stress ratio has been reported [54]. This effect is attributed to the plasticity induced crack closure [64]. This implies that the fracture surfaces developed in this region containing significant plastic flow. The striation marks are not continuously observed in this region. The modelling should be formulated that the effect of this plasticity or roughness induced fracture surface is reflected. It may be also assumed that the absence of striation marks revealed that striation is not created in one cycle and for these the plastic flow of material responsible for the striation marks are minute and cannot be detected. The model for FCG will be not the simple superimposition of monotonic and cyclic contribution for crack driving in this region.

5.1.2 Region II

This region is often termed as Paris region. The crack growth curve shape is less steep in this region and it is almost straight line on log-log, $\frac{da}{dN}$ vs ΔK plot. This region spans on a wider range of ΔK as shown in figure 5.1. The model developed in this thesis research work satisfactorily forecast crack growth in this region [63]. This implying that one cycle create one striation mark as show in figure 5.1. The stress ratio effect is adjusted into the two-parameter superposition model by default and as further correction is required for this effect. However, the case may vary from one material to another material due to composition difference. It is suggested that mechanistic model is developed in such a way that in region II, it is only the function of monotonic and cyclic load contribution superposition.

5.1.3 Region III

In region III the crack growth curve slope is sharp implying that it is more sensitive to the ΔK variation. In this region ΔK value approach K_c and non- stable growth is observed. The striation marks are generally not reported in literature for this region growth. The spacing and geometry of fractographic features is non -uniform in this region [44]. It is suitable to characterize crack growth in this region using static fracture criteria rather that fatigue fracture for which static fracture toughness can be used as prime parameter.

5.2 Fractographic features of the crack growth and mechanistic model

The fractographic features are important in the modelling of the fatigue growth. Literature studies are present where fractographic features are used for the development of

mechanistic model. The important fatigue fracture surface feature is striation marks, that has been extensively used for the development and understanding of the FCG model and fracture process respectively as shown in figure 5.2.
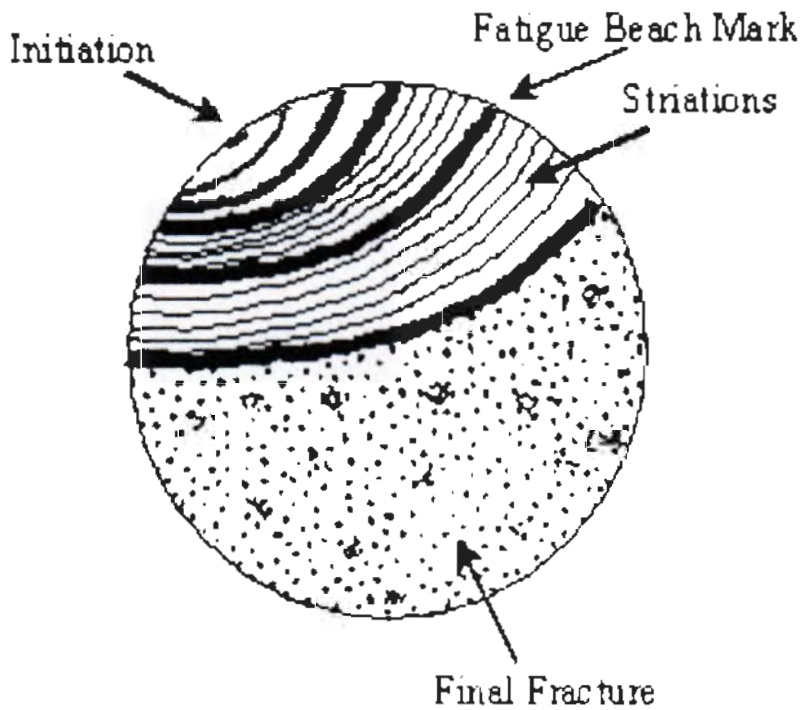
Figure 5.2: Fractographic features of fracture surface [65]

However, striation marks are not always observed for the whole SIF range and also for not all materials. Specifically, brittle materials don't exhibit striation due to absence of microplasticity during fracture. It is also still detectable weather striation marks are formed in single cycle or in multiple cycles since the famous models for striation formation are for one cycle [44,66]. This implies that more fracture features should he involved in the developing of mechanistic model for FCG. A good example of using extra fracture surface features is explored by the Khan's work [67] for composite delamination growth. Though their works is inherently for composites, the concept can be still extended to metal FCG. Moreover, the model of striation formation should be revised to realistically explain the phenomenon of fatigue fracture.

5.3 Similitude parameters for crack growth characterization

The fatigue spectrum is fully described by two loading parameters out of five parameters σ_{max}, σ_{min}, σ_{mean}, $\Delta\sigma$ and R as shown in figure 5.3.
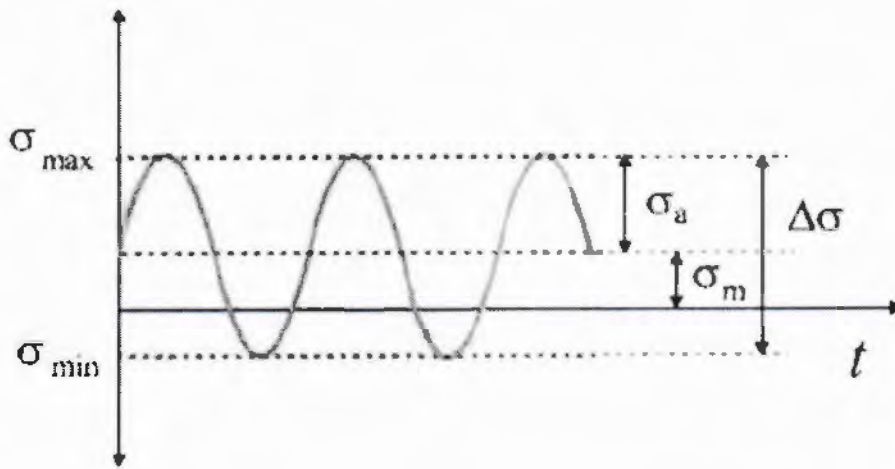
Figure 5.3: Loading history of fatigue [68]

The corresponding similitude parameters for FCG are K_{max}, K_{min}, K_{mean}, ΔK and R. In case of strain energy release rate (SERR), the parameters may be G_{max}, G_{min}, G_{mean}, ΔG and R. Researchers are widely divided in the use of a common parameters for FCG. The difference in approaches emanates from the foundation work of Paris equation. Whenever researchers observe that Paris equation was not able to predict FCG for different stress ratio and also different FCG regions, they used various above parameters for characterization. A unified parameter may be developed using the basics of thermodynamics energy conservation principles. An example of such work is Alderliesten [69] approach where the fracture energy required for new surface is related to the loading and from there a parameter has been developed. Further work is however needed to validate Alderliesten model.

CHAPTER 6

CONCLUSION AND FUTURE WORK

In this thesis at first, we survey the literature review about various models of FCG. Then we proposed a two-parameters model for FCG of metals in which the effects are superimposed monotonically and cyclically on the basis of latest approach about striation formation. Then the proposed two-parameter model has been validated by using authentic experimental literature review. The conclusions of the research work are summarized in section 6.1 and Future recommendation are presented in section 6.2.

6.1 Conclusion

➤ Striation marks are observed during our research and used by researcher for modelling.

➤ Striation marks relation with cyclic loading are clearly observed in Paris region.

➤ Two-parameters model fully predict the phenomenon instead of single parameter model.

➤ In Paris region superimposition model is effective for certain materials.

➤ In threshold region and region III striation marks are not observed so the proposed model doesn't predict this region.

➤ The proposed two-parameters model is just for Paris region.

6.2 Future recommendation

This research can be carried out in future considering the following effects:

➤ It should be needed to explore further the interaction of monotonic and cyclic loading and also include in the model to predict all the regions.

➤ The model of striation formation should be revised because it's doesn't accurate that one cycle creates one striation mark.

➤ As the striation marks are sometime observed and sometime not observed in threshold and region III so further fractographic features should be used for the modelling.

➤ For the characterization of region III static fracture should be used instead of fatigue fracture.

References:

[1] Schijve, J. (2001). *Fatigue of structures and materials*. Netherlands, Dordrecht: Kluwer Academic Publishers.

[2] Stephens, R. I., Fatemi, A., Stephens, R. R., and Fuchs, H. O. (2000). *Metal fatigue in engineering*. Canada, Toronto: A Wiley - Interscience Publishers.

[3] Grover, H.J. (1966). *Fatigue of aircraft structures*. U.S, Washington: Battelle Memorial Institute.

[4] Vethe, S. (2012). *Numerical Simulation of Fatigue Crack Growth*. Master's thesis, Institutt for produktutvikling og materialer.

[5] Beden, S. M., Abdullah, S., and Ariffin, A. K. (2009). Review of fatigue crack propagation models for metallic components. *European Journal of Scientific Research*, 28(3), pp. 364-397.

[6] Revankar, S.T., Wolf, B., and Roznic J. R. (2012). Metal Fatigue Crack Growth Models. *International Journal of Advanced Engineering Applications*, 1(4), pp. 85-91.

[7] Ritchie, R. (1979). Near-threshold fatigue-crack propagation in steels. *International Metals Reviews*, 24(1), pp. 205-230.

[8] Broek, D. (1974). Some contributions of electron fractography to the theory of fracture. *International Metallurgical Reviews*, 19(1), pp. 135-182.

[9] Paris, P. C., Tada, H., and Donald, J. K. (1999). Service load fatigue damage—a historical perspective. *International Journal of fatigue*, 21, pp. S35-S46.

[10] Tomkins, B. (1968). Fatigue crack propagation—an analysis. *Philosophical Magazine*, 18(155), pp. 1041-1066.

[11] Lal, D. and V. Weiss. (1978). A notch analysis of fracture approach to fatigue crack propagation. *Metallurgical Transactions A*, 9(3), pp. 413-426.

[12] Chan, K. and J. Lankford. (1983) A crack-tip strain model for the growth of small fatigue cracks. *Scripta Metallurgica*, 17(4), pp. 529-532.

[13] Suresh, S. (1983). Crack deflection: implications for the growth of long and short fatigue cracks. *Metallurgical Transactions A*, 14(11), pp. 2375-2385.

[14] McEvily, A. J., Eifler, D., and Macherauch. E. (1991). An analysis of the growth of short fatigue cracks. *Engineering Fracture Mechanics*, 40(3), pp. 571-584.

[15] Wu, X. J., Koul, A. K., and Krausz, A. S. (1993). A transgranular fatigue crack growth model based on restricted slip reversibility. *Metallurgical Transactions A*, 24(6), 1373.

[16] Bian, L. and Taheri, F. (2008). Analytical modeling of fatigue crack propagation in metals coupled with elasto-plastic deformation. *International journal of fracture*, 153(2), pp. 161-168.

[17] Schweizer, C., Seifert, T., Nieweg, B., Von Hartrott, P., and Riedel, H. (2011). Mechanisms and modeling fatigue crack growth under combined low and high cycle fatigue loading. *International journal of fatigue*, 33(2), pp. 194-202.

[18] Maierhofer, J., Pippan, R., and Gänser, H. P. (2014). Modified NASGRO equation for physically short cracks. *International Journal of Fatigue*, 59, pp. 200-207.

[19] Jiang, S., Zhang, W., Li, X., and Sun, F. (2014). An analytical model for fatigue crack propagation prediction with overload effect. *Mathematical Problems in Engineering*, 2014.

[20] Brown, M. W., and Miller, K. J. (1973). A theory for fatigue failure under multiaxial stress-strain conditions. *Proceedings of the Institution of Mechanical Engineers*, 187(1), pp. 745-755.

[21] Plumbridge, W. J., and Ryder, D. A. (1969). The metallography of fatigue. *Metallurgical Reviews*, 14(1), pp. 119-142.

[22] Ostash, O. P., and Panasyuk, V. V. (2003). A unified approach to fatigue macrocrack initiation and propagation. *International journal of fatigue*, 25(8), pp. 703-708.

[23] Ostash, O. P. (2006). New approaches in fatigue fracture mechanics. *Materials Science*, 42(1), pp. 5-19.

[24] Bian, L. C., Fawaz, Z., and Behdinan, K. (2006). A mixed mode crack growth model taking account of fracture surface contact and friction. *International journal of fracture*, 139(1), pp. 39-58.

[25] Lal, D. N. (1994). A mechanistic model for the influence of stress ratio on the LEFM fatigue crack growth behavior of metals and alloys—I. Crack-ductile materials. *Engineering fracture mechanics*, 49(6), pp. 871-897.

[26] De Los Rio, E. R., and Navarro, A. (1990). Considerations of grain orientation and work hardening on short-fatigue-crack modelling. *Philosophical Magazine A*, 61(3), pp. 435-449.

[27] Hussain, K., De Los Rios, E. R., and Navarro, A. (1993). A two-stage micromechanics model for short fatigue cracks. *Engineering Fracture Mechanics*, 44(3), pp. 425-436.

[28] Potirniche, G. P., and Daniewicz, S. R. (2003). Analysis of crack tip plasticity for microstructurally small cracks using crystal plasticity theory. *Engineering Fracture Mechanics*, 70(13), pp. 1623-1643.

[29]   Wen, W., and Zhai, T. (2012). Quantification of resistance of grain boundaries to short-fatigue crack growth in three dimensions in high-strength al alloys. *Metallurgical and Materials Transactions A, 43*(8), pp. 2743-2752.

[30]   Suresh, S. (1985). Fatigue crack deflection and fracture surface contact: micromechanical models. *Metallurgical and Materials Transactions A, 16*(1), pp. 249-260.

[31]   Taylor, D., Zakharov, M., and Bulatova. A. (1986). Fatigue of short cracks: the limitations of fracture mechanics. *In EGF pub 1.* pp. 479-490.

[32]   Lal, D. N. (1992). A model for the combined effects of stress ratio and grain size on the LEFM fatigue threshold condition. *Fatigue and Fracture of Engineering Materials and Structures, 15*(8), pp. 775-792.

[33]   McEvily, A. J., Endo, M., and Murakami. Y. (2003). On the relationship and the short fatigue crack threshold. *Fatigue and Fracture of Engineering Materials and Structures, 26*(3), pp. 269-278.

[34]   Endo, M., Sakai, H., and McEvily, A. J. (2006). An analysis of mode I fatigue crack growth under biaxial stress. *International Journal of Modern Physics B, 20*(25n27), pp. 3824-3829.

[35]   Chong-Myong, P., and Ji-Ho, S. (1994). Crack growth and closure behavior of short fatigue cracks. *Engineering fracture mechanics. 47*(3), pp. 327-343.

[36]   Wu, X., Deng, W., Koul, A., and Immarigeon. J. P. (2001). A continuously distributed dislocation model for fatigue cracks in anisotropic crystalline materials. *International journal of fatigue, 23*, pp. 201-206.

[37]   Chowdhury, P., and Sehitoglu, H. (2016). Mechanisms of fatigue crack growth–a critical digest of theoretical developments. *Fatigue and Fracture of Engineering Materials and Structures, 39*(6), pp. 652-674.

[38]   Wu, X. J., Wallace, W., Raizenne, M. D., and Koul, A. K. (1994). The orientation dependence of fatigue-crack growth in 8090 Al-Li plates. *Metallurgical and Materials Transactions A, 25*(3), pp. 575-588.

[39]   Bian, L. (2014). A new damage model and the prediction of elasto-plastic fatigue fracture. *Journal of Constructional Steel Research, 98*, pp. 114-122.

[40]   Metzger, M., Nieweg, B., Schweizer. C.. and Seifert, T. (2013). Lifetime prediction of cast iron materials under combined thermomechanical fatigue and high cycle fatigue loading using a mechanism-based model. *International Journal of Fatigue, 53.* pp. 58-66.

[41]   Dhopade, P., and Neely, A. J. (2014, June). Aeromechanical Modelling of Fan Blades to Investigate High-Cycle and Low-Cycle Fatigue Interaction. In *ASME Turbo Expo 2014: Turbine Technical Conference and Exposition*, Düsseldorf, 2014. Germany: American Society of Mechanical Engineers.

[42]   Dhopade, P., and Neely, A. J. (2015). Aeromechanical Modeling of Rotating Fan Blades to Investigate High-Cycle and Low-Cycle Fatigue Interaction. *Journal of Engineering for Gas Turbines and Power, 137*(5), pp. 052505-052505-12.

[43]   Kolitsch, S., Gänser, H. P., Maierhofer, J., and Pippan, R. (2016, March). Fatigue crack growth threshold as a design criterion-statistical scatter and load ratio in the Kitagawa-Takahashi diagram. In *IOP Conference Series: Materials Science and Engineering*. Leoben, 2016. Australia: IOP Publishing.

[44]   Nedbal, I., Siegl, J., Kunz, J., and Lauschmann, H. (2008). Fractographic reconstitution of fatigue crack history–Part I. *Fatigue and Fracture of Engineering Materials and Structures, 31*(2), pp. 164-176.

[45]   Laird, C., and Smith, G. C. (1962). Crack propagation in high stress fatigue. *Philosophical Magazine, 7*(77), pp. 847-857.

[46]   Laird, C. (1967). The influence of metallurgical structure on the mechanisms of fatigue crack propagation. In *Fatigue crack propagation*. ASTM International.

[47]   François, D., Pineau, A., and Zaoui, A. (1998). *Mechanical behavior of materials*. Dordrecht: Kluwer academic publishers.

[48]   Milella, P. P. (2013). Morphological aspects of fatigue crack formation and growth. In *Fatigue and Corrosion in Metals*, pp. 73-108. Springer Milan.

[49]   MILLS, W. J., and JAMES. L. A. (1980). Effect of temperature on the fatigue-crack propagation behavior of Inconel X-750. *Fatigue and Fracture of Engineering Materials & Structures, 3*(2), pp. 159-175.

[50]   Hertzberg, R. W. (1996). *Deformation and fracture mechanics of engineering materials*. Wiley.

[51]   Klingele, H. (1984, April). Essential features in fatigue fractures and remarkable phenomena in fatigue crack growth. *Fatigue Crack Topography*. Sienna, 1984. Italy: Specialised Printing Services Limited.

[52]   Bathias, C., and Pelloux, R. M. (1973). Fatigue crack propagation in martensitic and austenitic steels. *Metallurgical and Materials Transactions B, 4*(5), pp. 1265-1273.

[53]   Takeo, Y., and Kiyoshi, S. (1976). The effect of frequency on fatigue crack propagation rate and striation spacing in 2024-T3 aluminum alloy and SM-50 steel. *Engineering*

Fracture Mechanics, 8(1), pp. 81-88.

[54] Benachour, M., Benachour, N., and Benguediab, M. (2017, March). Fractographic Observations and Effect of Stress Ratio on Fatigue Striations Spacing in Aluminum Alloy 2024 T351. In *Materials Science Forum*, 887. pp. 3-8.

[55] Furukawa, K. (2000). Method for estimating service load from striation width and height. *Materials Science and Engineering: A, 285*(1), pp. 80-84.

[56] Lee, E. U., Glinka, G., Vasudevan, A. K., Iyyer, N., and Phan, N. D. (2009). Fatigue of 7075-T651 aluminum alloy under constant and variable amplitude loadings. *International Journal of Fatigue, 31*(11), pp. 1858-1864.

[57] Kearney, V. and R. Engle. (1967) Numerical analysis of crack propagation in cyclic loaded structures. *Journal of basic Engineering,* 89, pp. 459-64.

[58] Hörnqvist, M., Hansson, T., and Clevfors. O. (2010). Fatigue crack growth testing using varying R-ratios. *Procedia Engineering, 2*(1), 155-161.

[59] Perez, N. (2017). Introduction to fracture mechanics. In *Fracture Mechanics,* Switzerland, Cham, pp. 53-77. Springer International Publishing.

[60] Chang, T., and Guo, W. (1999). Effects of strain hardening and stress state on fatigue crack closure. *International journal of fatigue. 21*(9). pp. 881-888.

[61] Tsukuda, H., Ogiyama, H., and Shiraishi. T. (1995). Fatigue crack growth and closure at high stress ratios. *Fatigue and Fracture of Engineering Materials and Structures, 18*(4), pp. 503-514.

[62] Dubey, S., Soboyejo, A. B. O., and Soboyejo. W. O. (1997). An investigation of the effects of stress ratio and crack closure on the micro mechanisms of fatigue crack growth in Ti-6Al-4V. *Acta Materialia, 45*(7), pp. 2777-2787.

[63] Oberg, E., Jones, F. D., Horton, H. L., Ryffel, H. H., and Geronimo, J. H. (2004). *Machinery's handbook.* New York: Industrial Press New York.

[64] Toribio, J., and Kharin, V. (2013). Role of plasticity-induced crack closure in fatigue crack growth. *Frattura ed Integrit Strutturale.* 25(2013), pp. 130-137.

[65] Newman, J. C. (1998). The merging of fatigue and fracture mechanics concepts: a historical perspective. *Progress in Aerospace Sciences, 34*(5), pp. 347-390.

[66] Nedbal, I., Lauschmann, H., Siegl, J., and Kunz, J. (2008). Fractographic reconstitution of fatigue crack history–Part II. *Fatigue & Fracture of Engineering Materials & Structures, 31*(2), pp. 177-183.

[67] Khan, R., Alderliesten, R., and Benedictus, R. (2014). Two-parameter model for delamination growth under mode I fatigue loading (Part B: Model

development). *Composites Part A: Applied Science and Manufacturing*, *65*, pp. 201-210.

[68]   Suresh, S. (1998). *Fatigue of materials*. U.K, Cambridge: Cambridge university press.

[69]   Alderliesten, R. C. (2007). Analytical prediction model for fatigue crack propagation and delamination growth in Glare. *International Journal of Fatigue*, *29*(4), pp. 628-646.